ARTICLES
https://doi.org/10.1038/s41593-021-01001-5
nature neuroscience

Prepubescent female rodents have enhanced hippocampal LTP and learning relative to males, reversing in adulthood as inhibition increases

Aliza A. Le[1], Julie C. Lauterborn[1], Yousheng Jia[1], Weisheng Wang[1], Conor D. Cox[1], Christine M. Gall[1,2] ✉ and Gary Lynch[1,3] ✉

Multiple studies indicate that adult male rodents perform better than females on spatial problems and have a lower threshold for long-term potentiation (LTP) of hippocampal CA3-to-CA1 synapses. We report here that, in rodents, prepubescent females rapidly encode spatial information and express low-threshold LTP, whereas age-matched males do not. The loss of low-threshold LTP across female puberty was associated with three inter-related changes: increased densities of α5 subunit-containing $GABA_A$Rs at inhibitory synapses, greater shunting of burst responses used to induce LTP and a reduction of NMDAR-mediated synaptic responses. A negative allosteric modulator of α5-$GABA_A$Rs increased burst responses to a greater degree in adult than in juvenile females and markedly enhanced both LTP and spatial memory in adults. The reasons for the gain of functions with male puberty do not involve these mechanisms. In all, puberty has opposite consequences for plasticity in the two sexes, albeit through different routes.

There is considerable evidence for sex differences in learning. Among adults, men generally score higher on spatial problems, whereas women are frequently better on semantic tests[1,2]. Although, for some tasks, differences have been shown to reflect sex-specific learning strategies, and other influences including task familiarity, mode of testing and task demands[3–8], the disparity in spatial learning has been reported for diverse species of mammals, suggesting that it might be a characteristic feature of the class[9]. Relatedly, sex differences in forms of synaptic plasticity underlying learning have been described. In hippocampal field CA1, LTP is dependent on locally synthesized estrogen in females but not in males[10]. The rate-limiting enzyme (p450 aromatase) for synthesis of estradiol (E2), the most prevalent and potent estrogen in brain, is present at high levels in hippocampus and localized to axon terminals[11–13], and E2 levels are several-fold higher in hippocampus than in blood in both sexes[14,15]. However, blocking E2 synthesis disrupts LTP only in females[10,16]. Moreover, at hippocampal CA3-to-CA1 synapses, released estrogen acts through estrogen receptor α (ERα) to activate the LTP critical kinases ERK1/2 and Src, and BDNF receptor TrkB, in females but not in males[16]. It, thus, appears that females require locally produced estrogen to induce critical synaptic modifications, whereas males do not. Parallel studies found that the minimum afferent stimulation needed to elicit LTP (the LTP threshold) is greater in adult females than males[16], an effect that is plausibly related to the addition of an estrogen-dependent step in the sequence for inducing potentiation. Given the central role of hippocampus in spatial learning, the higher female LTP threshold helps explain why, in rodents, adult females require more training to learn object location than age-matched males[16].

The present studies tested if the elevated LTP and learning thresholds identified in female rodents are products of late development. Puberty is a critical landmark in brain maturation and results in a wide array of sex differences in behavior[17–19], but little is known about how it affects the substrates for memory encoding. Past studies showed that, in male rats, the magnitude of LTP reaches adult levels by the end of the fourth postnatal week and, thus, in advance of puberty[20–22]. However, these studies did not assess LTP threshold, which is more closely related to neuronal activity occurring during behavior. Studies addressing developmental changes in LTP in female rodents are rare[23], and none have compared the sexes. Thus, it is possible that the sex differences described above are absent or different in prepubertal animals. Such sexually differentiated adjustments during puberty are known to occur in certain psychological domains; anxiety attacks and depression, which occur more frequently in postpubescent girls than boys, are prominent examples[24–26]. Results described here indicate that the transition from prepubertal to postpubertal life causes strikingly different and, indeed, opposite male versus female changes in LTP and associated spatial learning. They also describe synaptic mechanisms related to the marked developmental changes that occur in females.

Results

Hippocampal LTP threshold before versus after puberty. We used theta burst stimulation (TBS) to induce potentiation of Schaffer commissural (SC) afferents to field CA1 in acute hippocampal slices from prepubescent (postnatal day (P) 21–28) and young adult (2–3-month-old) rats. The amplitudes of field excitatory post-synaptic potentials (fEPSPs) elicited in the CA1 apical dendrites by single-pulse stimulation of SC projections were tightly related to the amplitudes of the preceding fiber volley. Input–output (fiber volley versus fEPSP amplitude) curves were similar between ages and sex (Fig. 1a). Previous studies using multiple short trains of three bursts, a protocol that is near threshold for eliciting stable potentiation[27], identified a marked sex difference in SC LTP threshold[16].

[1]Department of Anatomy and Neurobiology, University of California, Irvine, Irvine, CA, USA. [2]Department of Neurobiology and Behavior, University of California, Irvine, Irvine, CA, USA. [3]Department of Psychiatry and Human Behavior, University of California, Irvine, Irvine, CA, USA.
✉e-mail: cmgall@uci.edu; ga.s.lynch@gmail.com

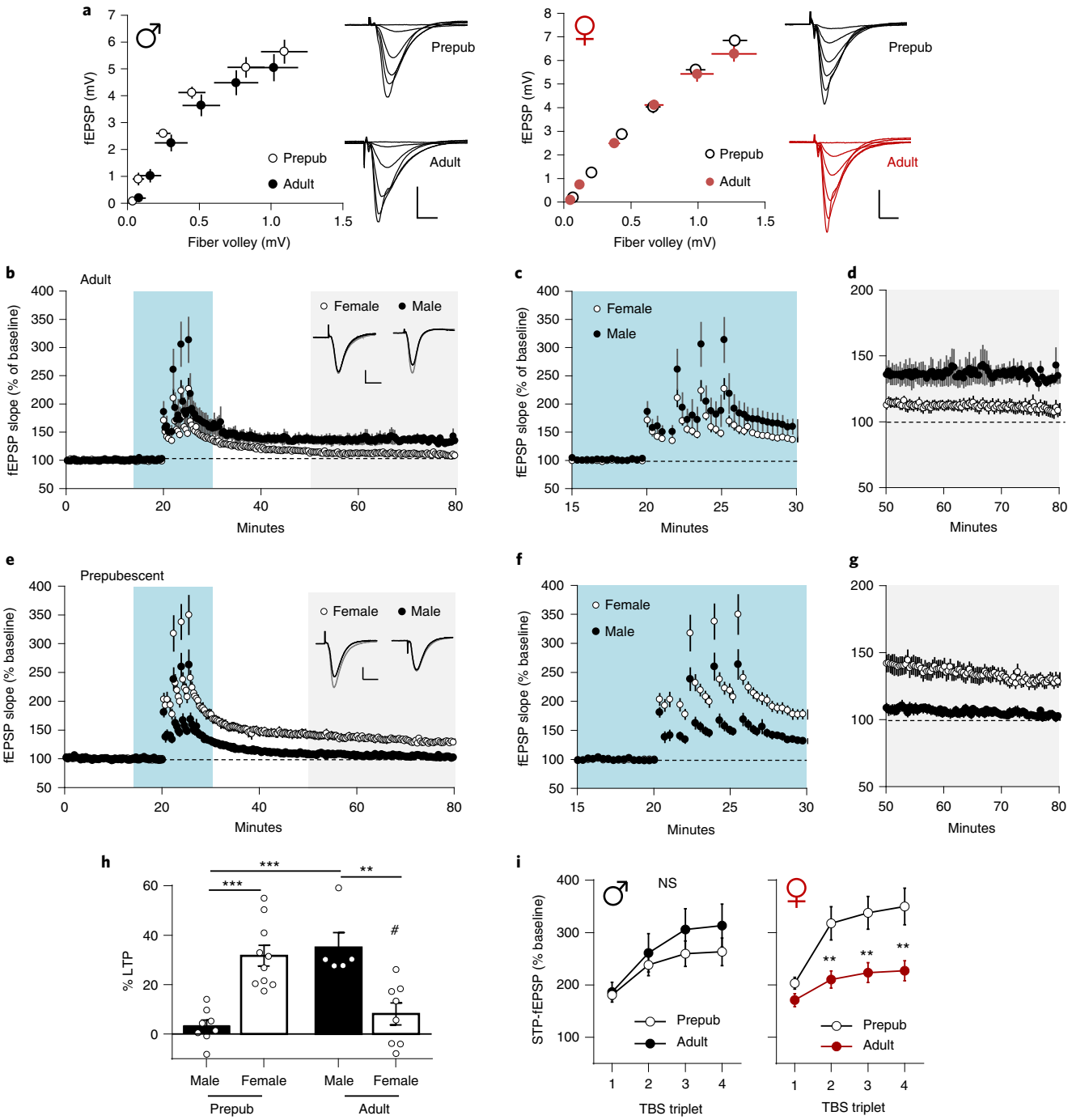

Fig. 1 | Sex differences in adult rat LTP thresholds are reversed before puberty. fEPSPs elicited by stimulation of the SC projections were recorded in CA1 stratum radiatum in acute hippocampal slices from prepubertal ('Prepub'; 3–4 week) and adult (8–10 week) rats of both sexes. **a**, Input–output curves were similar across age and sex ($P = 0.46$, $F_{3,124} = 0.86$, linear regression). Representative traces on right. Bars: 2 mV, 5 ms. **b**, Four theta burst 'triplets', spaced by 90 s, were delivered to SC axons after 20 min of baseline. Each triplet included three bursts (one burst: four pulses at 100 Hz) separated by 200 ms. After the triplets, single-pulse responses in adult females decayed steadily to baseline, whereas those in males fell to a stable plateau just above baseline values. Inset: superimposed traces from baseline (black) and the end of the recording session (gray). Bars: 1 mV, 10 ms. **c**, Stretched *x* axis (minutes 15–30 of **b**) to illustrate single-pulse responses during the 90 s after each triplet; male fEPSPs were elevated above those of females, indicating a sex difference in STP. **d**, Stretched axes (minutes 50–80 of **b**) show that adult males had a lasting increase in fEPSPs after TBS, whereas females did not. **e**–**g**, Same format as that for **b**–**d** but for prepubescent rats. Responses recorded for 90 s after each triplet are much larger in females than males (**f**), the reverse of the pattern recorded in adults, and females expressed robust LTP, whereas males did not (**g**). **h**, Summary of LTP (55–60 minutes post-induction) for both age groups and sexes (two-way ANOVA interaction: $F_{1,25} = 36.35$, $P = 0.00005$; Tukey post hoc: $^{***}P < 0.001$, $^{**}P < 0.01$, $^{\#}P = 0.0015$ for adult female versus prepubescent female). **i**, Averaged fEPSP slope responses (percent baseline) collected after each of the four theta burst triplets. There was no reliable difference for STP in prepubescent versus adult male slices (two-way repeated-measures ANOVA: $F_{3,33} = 1.781$, $P = 0.17$), but STP was larger in prepubescent female versus adult female slices ($F_{3,42} = 11.57$, $P = 8.44 \times 10^{-6}$; Bonferroni post hoc: $^{**}P < 0.01$). For all panels, $n = 5$–10. Mean ± s.e.m. values are shown. Statistics are summarized in Supplementary Table 1. NS, not significant.

We compared effects of four such triplets, applied at 90-s intervals, on prepubertal versus postpubertal slices. LTP was obtained in adult males but not females (Fig. 1b); the percent potentiation at 55–60 min after induction was 35.0 ± 6.1% and 8.1 ± 4.4%, respectively ($P = 0.0038$, unpaired t-test). The sex difference was also present in short-term potentiation (STP) recorded during the 90 s after each triplet ($F_{3,33} = 7.40$, $P = 0.0006$, repeated-measures ANOVA; Fig. 1c). After the last triplet, potentiation steadily decayed to baseline in females but not in males (Fig. 1d).

Results for the prepubescent groups were substantially different than those for adults: theta burst triplets induced robust LTP in females (29.2 ± 4.6% at 55–60 min after induction) but not in males (3.9 ± 2.7%; unpaired t-test: $P = 0.0005$) (Fig. 1e). Sex differences were also evident for STP ($F_{3,42} = 4.181$, $P = 0.01$, repeated-measures ANOVA; Fig. 1f). Potentiation was sustained over the subsequent 40 min in females, whereas the smaller effect in males quickly fell to baseline (Fig. 1g). In all, theta bursts produced a more pronounced initial potentiation in prepubescent females than in age-matched males and is reflected in the magnitude and stability of subsequent LTP.

Results above indicate that, with age, SC LTP threshold changes in opposite directions for males versus females. The difference in percent potentiation at 55–60 min after induction for pre-puberty versus post-puberty groups was highly significant for both sexes (two-way ANOVA: $F_{1,25} = 36.35$, $P < 0.0001$; Tukey post hoc: female: $P = 0.0015$, male: $P = 0.0004$) (Fig. 1h). Burst triplets produced substantially greater STP before than after puberty in females (repeated-measures ANOVA: $F_{3,48} = 11.57$, $P < 0.0001$) (Fig. 1i, right). By contrast, STP in males tended to be smaller before than after puberty, but this was not statistically significant ($F_{3,33} = 1.78$, $P = 0.17$; Fig. 1i, left). These results raise the possibility that the brief post-synaptic depolarization produced by theta bursts decreases with female puberty, resulting in an increase in the number of bursts needed to produce LTP, and that male changes across puberty are likely to involve other types of mechanisms.

Spatial learning thresholds before versus after puberty. The LTP threshold data (above) lead to the striking prediction that the male–female differences in minimum cue exposure required for spatial memory in young adults would be reversed before puberty. We tested this using threshold duration training in the Object Location Memory (OLM) task (Fig. 2a), a paradigm in which memory is CA1 dependent and facilitated by E2[28–30].

Prepubescent (P25) and adult (2–3 months) male and female mice were given an initial 5-min exposure to two identical objects ('training' session) and, 24 h later, a 5-min 'testing' session during which they re-explored the arena with one object displaced toward the center. Despite lacking high levels of circulating estrogen[31], prepubescent females preferentially explored the novel location object during testing, as indicated by high Discrimination Index (DI) scores, whereas adult females trained during low-estrogen states ('non-proestrus') showed no preference (low DI scores) (Fig. 2b). The opposite developmental pattern held for males: adults performed significantly better than prepubertal mice. When comparing sexes in age-matched mice ($F_{1,56} = 27.07$, $P < 0.0001$, interaction two-way ANOVA), adult males outperformed adult females ($P = 0.003$, Tukey post hoc), whereas prepubescent females scored better than prepubescent males ($P = 0.002$). As predicted from the DI scores, prepubescent females and adult males both explored the novel location object more than the familiar location object (paired t-tests: $P = 0.0001$ for females, $P = 0.0006$ for males), whereas adult, non-proestrus females and prepubescent males did not ($P = 0.21$ and $P = 0.73$, respectively; Extended Data Fig. 1a). As described[16], adult females trained during the high-estrogen stage (proestrus) showed a marked preference for the novel location object ($P = 0.004$; Extended Data Fig. 1b).

In contrast to the above, adult females given 10 min (as opposed to 5 min) of training discriminated the novel location object during testing ($P = 0.01$), indicating that they require longer training than prepubescent females to encode spatial memory. Surprisingly, prepubescent males given extended (10-min) training still did not discriminate the moved object ($P = 0.46$; Extended Data Fig. 1b).

Next, we tested if the lower facility for rapid spatial learning in prepubescent males and adult females involves problems related to initial acquisition of cue locations as opposed to later consolidation of the information. Mice were given 5-min training sessions and tested for OLM 15 min later (Fig. 2a). The DI for non-proestrus adult females was near 0, indicating that they failed to develop short-term memory for object location. In contrast, although prepubescent males did not encode long-term memory for cue location as assessed at 24 h, they had excellent DIs after the short delay (adult female versus prepubescent male; $P = 0.0002$, unpaired t-test) (Fig. 2c and Extended Data Fig. 1c). These data reinforce the conclusion from the STP analyses in the physiological experiments that the reversal of sex differences across puberty is due to different types of changes in female versus male plasticity.

Total cue sampling times (both objects) during OLM training and testing were greater for adult than prepubescent mice (females: $P \leq 0.0002$, males: $P \leq 0.0012$) but did not differ between the sexes at either age (Supplementary Fig. 1a,b). Thus, the absence of long-term memory in adult females was not due to a failure to investigate the objects and their locations. Inattention could, however, have been a factor in the poor performance by prepubescent males (but see below). There were no evident differences between groups in locomotor activity in the behavioral sessions (Supplementary Fig. 1c).

The above findings raise the question of whether differences in spatial learning are specific to simple tasks such as OLM or instead occur in the same subgroups in more complex circumstances. We tested this using a paradigm in which mice freely sampled four distinct and equally salient odors for 5 min and were tested for preferences 24 h later with positions of two of the odors swapped ('Where' task; Fig. 2d). Note that the animals sequentially investigate a collection of cues under these circumstances and that recognition of changes requires encoding of both cue location and identity. Thus, the task is considerably more challenging than OLM and incorporates both 'What' and 'Where' features of episodic memory. The animals sampled the four odors to a similar degree during training with no evident differences between groups (Extended Data Fig. 1d). The DI indicated that adult, non-proestrus females did not discriminate the novel location cues at testing, whereas prepubescent females spent significantly more time with moved odors (Fig. 2e) ($P = 0.008$, paired t-test; Extended Data Fig. 1e). Males exhibited the opposite pattern: prepubescent males had a DI near 0, whereas adults preferentially attended to the moved cues (Fig. 2e). A two-way ANOVA ($F_{1,34} = 21.38$, $P < 0.0001$) of the four groups showed that the adult females and prepubescent males performed worse than the other two groups ($P \leq 0.043$, Tukey post hoc).

In contrast to the OLM results, there were no age or sex differences in the total time spent investigating the four odors during training or testing for the episodic 'Where' task (Supplementary Fig. 1d,e). Thus, in this case, the absence of long-term memory in postpubescent females and prepubescent males cannot be attributed to different sampling times. There were no evident differences in locomotion during behavioral sessions (Supplementary Fig. 1f).

We then tested additional groups to determine if there are sex or age differences in a version of the multi-cue task with a minimal spatial component (episodic 'What' test). Mice were allowed to sample four odors for 5 min and were tested 24 h later with one of the cues replaced by a novel odor (Fig. 2d and Extended Data Fig. 1f). In contrast to results for the combined cue identity–location problem, all four groups showed a clear preference for the novel odor at testing (Fig. 2f and Extended Data Fig. 1g). Total sampling times

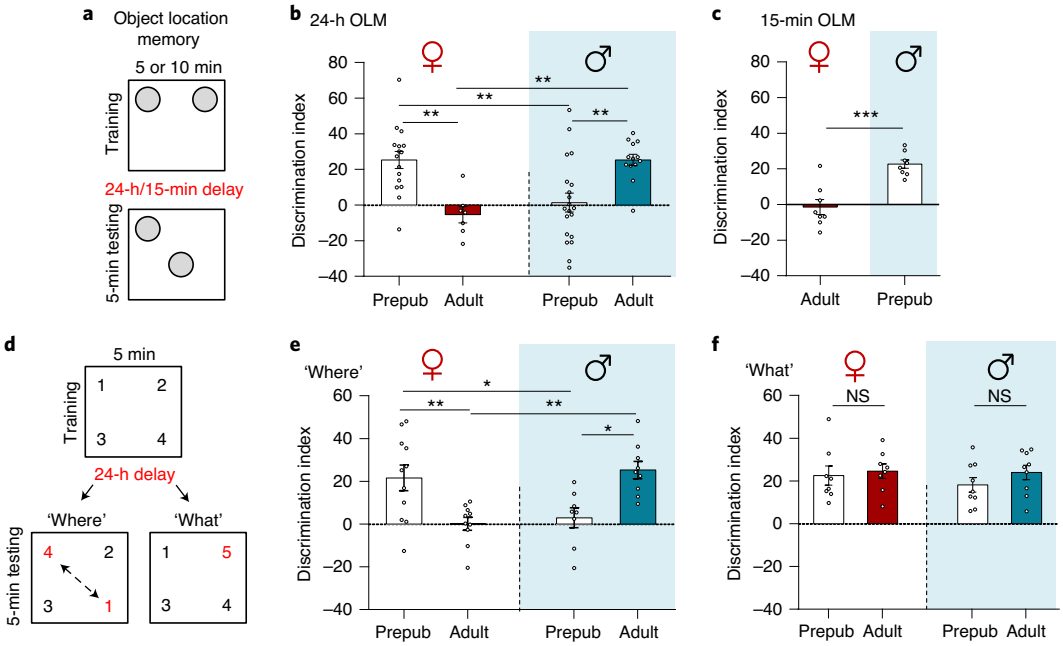

Fig. 2 | Adult sex differences in spatial learning are reversed before puberty. a, OLM paradigm. Mice were exposed to two identical objects for 5 min ('training'). After a delay, mice were returned to the chamber for 5 min with one object displaced ('testing'). **b**, With a 24-h delay, prepubescent ('Prepub') females ($n=16$) discriminated the displaced object, whereas adult females ($n=7$) (two-way ANOVA (interaction of sex and age): $F_{1,56}=27.07$, $P=2.9\times10^{-6}$; Tukey post hoc: $^{**}P=0.0034$) and prepubescent males ($n=20$) ($^{**}P=0.002$) did not. Conversely, adult males ($n=17$) better discriminated the moved object than prepubescent male ($^{**}P=0.0016$) and adult female ($^{**}P=0.003$) mice. **c**, When tested 15 min after training, adult females performed significantly worse in the task than prepubescent males (two-tailed unpaired *t*-test: $^{***}P=0.0002$, $n=8$ per group). **d**, Episodic 'Where' and 'What' task schematic. Mice were exposed to four different odors for 5 min (training); 24 h later, the animals explored the chamber with either two objects switched in position ('Where') or one odor replaced by a novel odor ('What'). **e**, In the 'Where' task, prepubescent females better discriminated the switched odor pairs than did adult females ($F_{1,34}=21.38$, $P=5.25\times10^{-5}$; Tukey post hoc: $^{**}P=0.0091$) and prepubescent males ($^{*}P=0.043$). Adult males better discriminated switched odors than prepubescent males ($^{*}P=0.016$) and adult females ($^{**}P=0.003$) ($n=8$–11 per group). **f**, In the 'What' task, all groups preferentially explored the novel odor versus the familiar odors at testing ($F_{1,30}=0.26$, $P=0.61$, $n=8$–9 per group). Mean ± s.e.m. values are shown. Statistics are summarized in Supplementary Table 1. NS, not significant.

were similar to those for OLM in that adult males and females sampled the cues longer than their prepubescent counterparts (Supplementary Fig. 1h), but this did not appear to influence retention scores. Locomotor activity was similar between groups (Supplementary Fig. 1i). These findings establish that sex and age do not significantly affect encoding cue identity but that changes across puberty produce opposite effects on female versus male learning when a spatial component is introduced.

Factors relating to the developmental changes in female LTP. The STP results described above could reflect age and sex differences in the depolarizing responses produced by theta burst triplets and, thus, the likelihood of triggering the initial steps leading to LTP. Comparisons of the composite response to a single four-pulse theta burst in rat slices confirmed that the amplitudes of the second–fourth fEPSP were substantially larger in females before versus after puberty ($F_{3,90}=24.40$, $P=5.38\times10^{-12}$, repeated-measures ANOVA) (Fig. 3a). These results are suggestive for underlying mechanisms. Afferents from CA3 monosynaptically innervate both CA1 pyramidal cells and local interneurons, some of which form inhibitory synapses in the same dendritic field (stratum radiatum) as the excitatory contacts[32]. Inhibitory post-synaptic currents (IPSCs) are slower than the fast AMPAR-mediated glutamatergic currents and, thus, exert their greatest shunting effects on EPSCs triggered by the third and fourth pulses in a theta burst[33,34].

We tested the possibility of an age-related increase in feed-forward IPSCs in females using voltage-clamp recordings to compare effects of the $GABA_AR$ antagonist bicuculline on the size of a burst response in prepubescent and adult rat slices (Fig. 3b). In agreement with the field recordings, the area of the baseline (pre-drug) burst response, normalized to the amplitude of the first EPSC in the burst, was nearly twice as large in prepubertal females (60.6 ± 2.8 pA × ms) as in adult females (31.3 ± 3.6 pA × ms; $P=0.0002$, unpaired *t*-test). The burst response area tended to decrease with age in males (pre-puberty versus post-puberty: 61.4 ± 3.5 vs. 51.0 ± 4.3 pA × ms), but this effect did not reach statistical significance ($P=0.068$, unpaired *t*-test; Supplementary Fig. 2a). The percent decrease from prepubescence to adulthood was significantly larger in females (−48.3 ± 5.9%) than in males (−16.9 ± 7.1%) ($P=0.004$, unpaired *t*-test). Bicuculline had a larger effect after puberty: in females, it increased the area of a single burst response by 82.5 ± 22.9% and 195.8 ± 29.7% in prepubescent and adult animals, respectively ($P=0.02$, unpaired *t*-test) (Fig. 3c). The antagonist had a measurably greater effect on normalized burst responses in males than females before ($P=0.019$, unpaired *t*-test) but not after ($P=0.273$) puberty. These results indicate that feed-forward IPSCs during a burst response increase across puberty in females and, thereby, more potently shunt the depolarization produced by a burst in adults.

Delivery of two bursts separated by 150–200 ms results in a marked facilitation of the second response due to partial suppression of feed-forward IPSPs[35,36]. The enhanced and prolonged depolarization unblocks NMDARs and, thus, initiates the sequence leading to the production of LTP[37]. We used the selective NMDAR antagonist APV to estimate the magnitude of the NMDAR component of the burst response before versus after female puberty. A pair of theta bursts was delivered under control conditions and

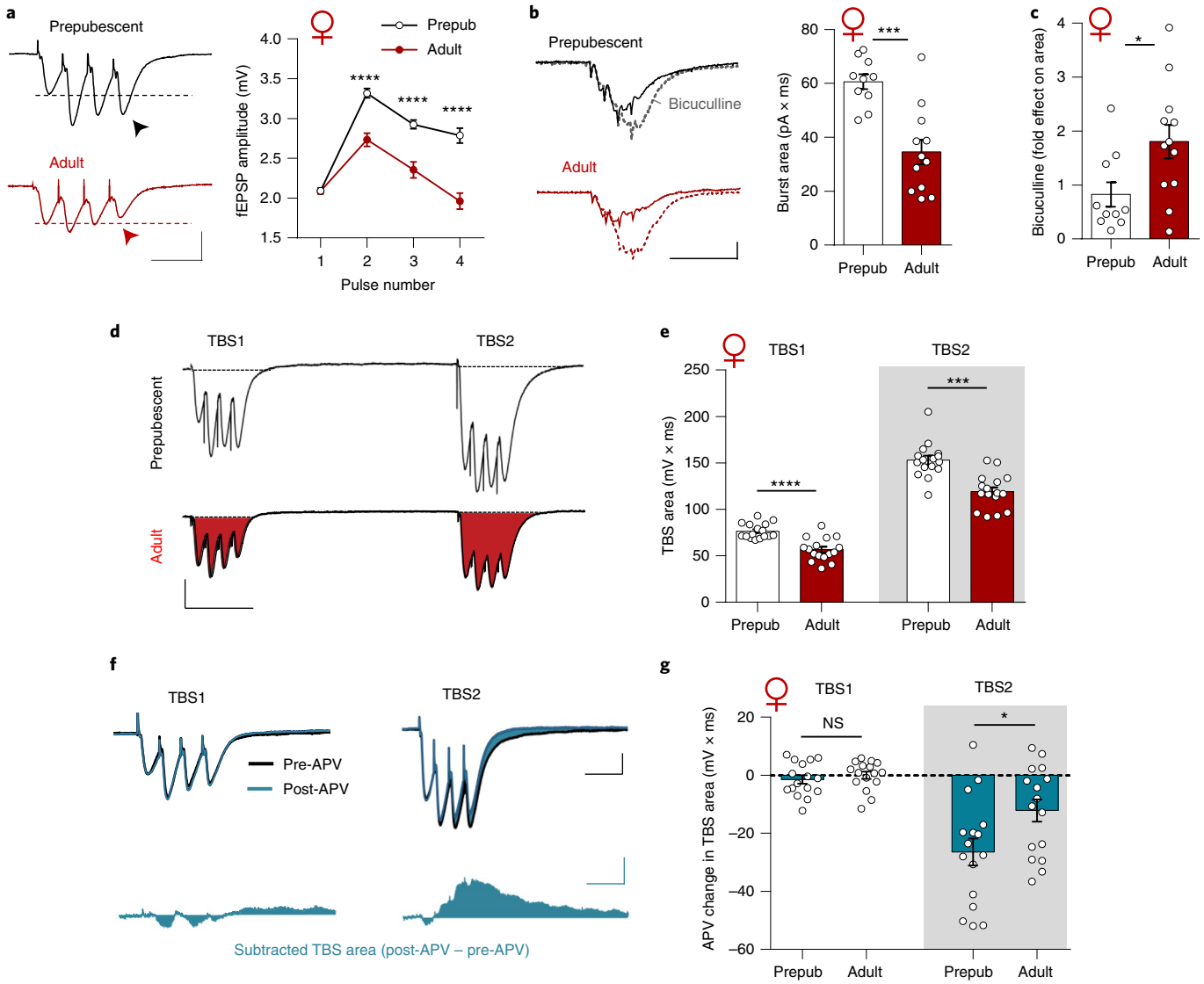

Fig. 3 | Theta burst responses, feed-forward inhibition and NMDAR-mediated synaptic potentials differ between prepubescent and postpubescent female rats. a, Traces of fEPSP responses elicited by a single burst (four pulses, 100 Hz) delivered to the SC projections and recorded from CA1 stratum radiatum in slices from prepubescent ('Prepub') or adult female rats. Arrowheads mark the fourth fEPSP in the burst response. Bars: 2 mV, 20 ms. Right: Graph shows the four fEPSPs within the burst responses in adult and prepubescent groups (two-way repeated-measures ANOVA, $F_{3,90} = 25.40$, $P = 5.38 \times 10^{-12}$. Asterisks indicate group differences for each fEPSP in the burst response: Bonferroni post hoc, $^{****}P < 0.0001$). **b**, Voltage-clamp recordings from CA1 pyramidal cells during delivery of single-burst stimulation to SC projections in slices from prepubescent or adult female rats before (solid trace) and during (dotted) infusion of bicuculline (20 μM, 10 min). In adults, the baseline response is smaller, and the $GABA_AR$ antagonist had a greater effect (bars: 100 pA, 50 ms). Graph shows areas of baseline (pre-drug) burst responses for prepubescent ($n = 10$) and adult ($n = 12$) groups: the size of the composite four EPSC responses (normalized to amplitude of the first response) was nearly twice as large in prepubescent versus adult females (two-tailed unpaired *t*-test: $^{***}P = 0.0002$). **c**, Group data for effects of bicuculline before versus after puberty. The antagonist had substantially larger effect in slices from the older rats (two-tailed unpaired *t*-test: $^{*}P = 0.02$). **d**, Traces show SC responses elicited by two theta bursts (four pulses at 100 Hz, 200-ms interval) in prepubertal and adult female slices (bars: 1 mV, 50 ms). **e**, Group data for areas of responses elicited by the first and second theta bursts. As in **a**, the first of these (TBS1) was larger in prepubertal slices than in adult female slices (two-tailed unpaired *t*-test: $^{****}P = 7.4 \times 10^{-6}$); this was also the case for the composite response to the second burst (TBS2) ($^{***}P = 0.0003$). **f**, Traces show superimposed theta burst responses before and after 30-min infusion of NMDAR antagonist APV (100 μM) (bars: 1 mV, 25 ms). The bottom graphs (solid blue) show the results of subtracting the baseline responses to TBS1 and TBS2 from those recorded in the presence of APV (bars: 0.5 mV, 25 ms). Note that APV reduced the later segments of the negative-going response to TBS2 while having minimal effects on that produced by TBS1. **g**, Summary of group data for effects of APV on the size of responses to two theta bursts: APV did not alter the composite response to TBS1 in prepubescent or adult slices (NS $P = 0.46$) but reduced the areas of responses to TBS2. The attenuation of the TBS2 response was larger before puberty ($^{*}P = 0.024$, two-tailed unpaired *t*-test). For **a**,**e**,**g**: $n = 16$ per group. Data are presented as mean values ± s.e.m. NS, not significant.

then again after 30 min of APV infusion. As expected from above, the area of the composite potential produced by the first (control) theta burst was substantially larger in slices from prepubertal than adult female rats ($P < 0.0001$) (Fig. 3d,e). Notably, the amplitude of the initial fEPSP within the burst was virtually identical in the two groups (Prepuberty: 2.10 ± 0.02 mV, Adult: 2.11 ± 0.03 mV;

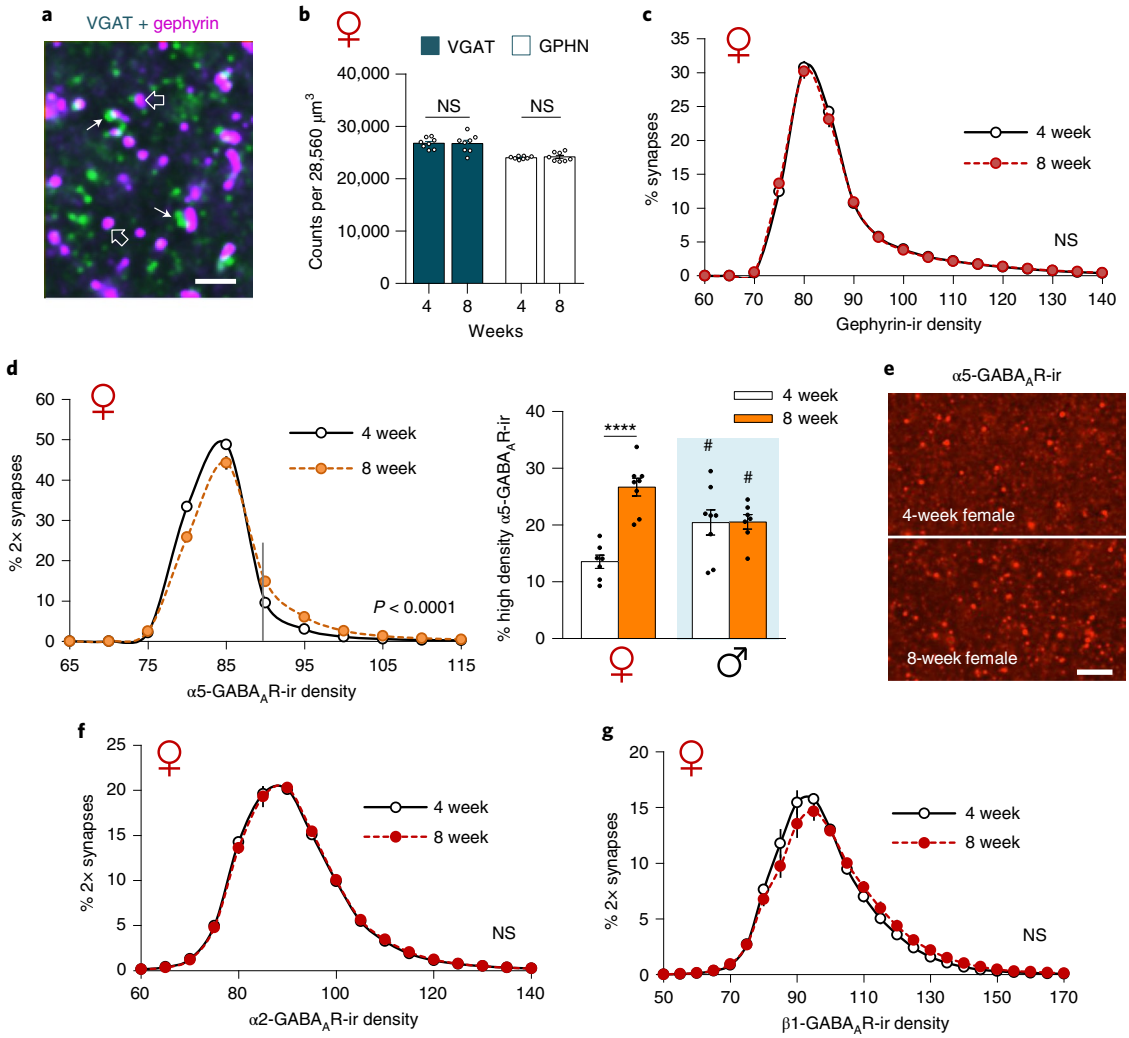

Fig. 4 | Synaptic levels of $GABA_AR$ subunits in prepubescent versus postpubescent female rats. a–c, Dual immunofluorescence for pre-synaptic VGAT and post-synaptic gephyrin (GPHN) in CA1 stratum radiatum indicates that numbers of inhibitory synapses are equivalent in the two age groups. **a**, Image shows immunofluorescence localization of GPHN (open arrows, magenta) and VGAT (closed arrows, green) in an 8-week-old female. Calibration bar, 2 µm. **b**, Counts of VGAT-immunoreactive (-ir) and GPHN-ir puncta (mean ± s.e.m.) were similar at 4 and 8 weeks of age (two-tailed unpaired *t*-test: VGAT, $P=0.92$; GPHN, $P=0.78$). **c**, Immunolabeling density frequency distributions for GPHN-ir elements did not differ between groups ($F_{40,560}=0.58$, $P=0.98$). **d**,**e**, The density of immunolabeling for the α5-$GABA_AR$-ir at inhibitory synapses changes from 4 to 8 weeks in females but not in males. **d**, Left: Plot shows the density frequency distributions for α5-ir co-localized with GPHN ('2× synapses') in females: the curve for the 8-week group was markedly right-shifted toward higher densities relative to that for the 4-week group ($P=5.8\times10^{-78}$, $F_{50,700}=14.46$). Right: Graph shows the percentage of double-labeled synapses with dense α5-ir (above vertical cutoff line on the frequency distribution curve) in female and male rats (Supplementary Fig. 2b for male frequency distribution). Values were significantly higher in postpubescent versus prepubescent females, whereas males showed no change between ages (two-way ANOVA interaction: $F_{1,26}=15.30$, $P=0.0006$; Tukey post hoc: $^{****}P<0.0001$ and $^{\#}P<0.05$ versus 4-week female; $P=0.99$ for 4-week versus 8-week male). **e**, Photomicrographs of α5-$GABA_AR$-ir in CA1 stratum radiatum illustrate the increase in densely immunolabeled puncta in 8-week-old versus 4-week-old females. Bar, 5 µm. **f**,**g**, Density frequency distributions for α2-$GABA_AR$-ir (**f**) and β1-$GABA_AR$-ir (**g**) show that levels of synaptic immunoreactivity (co-localized with GPHN) did not differ between prepubescent and postpubescent females (α2: $P>0.99$, $F_{50,700}=0.17$; β1: $P=0.07$, $F_{50,700}=1.32$). For all panels, $n=7$–8 per group. Statistics in **c**,**d**,**f**,**g** were performed with two-way repeated-measures ANOVA (interaction). Data are presented as mean values ± s.e.m. NS, not significant.

$P=0.64$, unpaired *t*-test), indicating that the age difference in burst responses was due to the second–fourth potentials. The prepubescent cases also had a larger response to the second theta burst than did adults during baseline testing (159.9 ± 4.8 versus 119.1 ± 4.7 mV × ms, respectively; $P=0.0003$) (Fig. 3e). After APV infusion, the response to the first of the two theta bursts was not measurably different than that before APV infusion for either age group, but the magnitude of the second burst response was reduced in both cases. We subtracted the waveforms of the APV-plus responses from those acquired before APV infusion to quantify the drug effect (Fig. 3f). This analysis confirmed that the antagonist had no effect on the first burst response but removed a significant component of the second, an effect that was clearly greater in pre-puberty versus post-puberty slices (−26.4 ± 4.6 versus −12.1 ± 3.8 mV × ms, respectively; $P=0.024$) (Fig. 3g). This accorded with the prediction that the NMDAR-mediated component of the composite response decreases across puberty in females.

$GABA_AR$ synapses before versus after female puberty. The above findings indicate that some element of fast ionotropic GABAergic

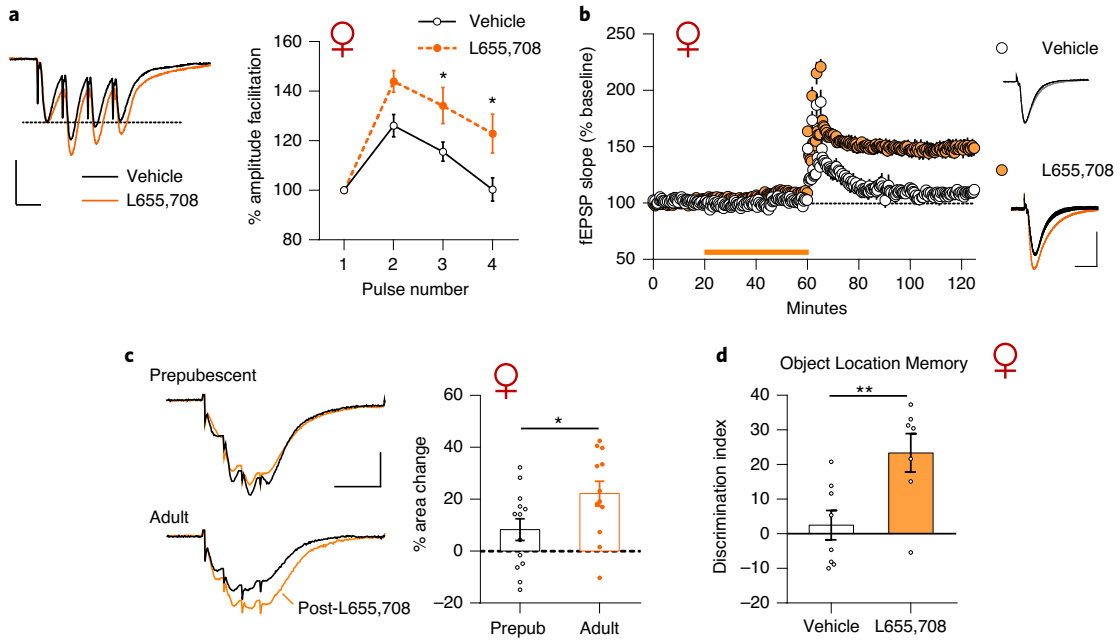

Fig. 5 | A NAM (L655,708) of the α5-GABA$_A$R subunit increases theta burst responses and facilitates LTP in adult females. a,**b**, Baseline responses were collected for 20 min before a 40-min infusion of L655,708 (150 nM) in adult female rat hippocampal slices. Four TBS 'triplets' (90-s intervals) were applied to induce LTP after drug treatment. **a**, Left: L655,708 increased the size of the response to one theta burst (four pulses, 100 Hz) relative to vehicle treatment (bars: 2 mV, 10 ms). Right: Group data ($n=7$–8 per group) for the four fEPSP amplitudes normalized to the first pulse that comprise a single theta burst response (two-way repeated-measures ANOVA: $P=0.011$, $F_{3,39}=4.21$; Bonferroni post hoc (third pulse: $^{*}P=0.048$ and fourth pulse: $^{*}P=0.012$)). **b**, Female slices treated with L655,708 (line bar) express robust LTP, whereas those infused with vehicle do not (two-tailed unpaired *t*-test: $P=0.0002$ at 1 h after TBS; $n=7$ per group). Right, representative superimposed traces. Black: baseline; orange: after LTP; bars: 2 mV, 10 ms. **c**, Voltage-clamp recordings from CA1 neurons elicited by a single theta burst from prepubescent versus adult female mouse slices before (black trace) and during infusion with L655,708 (50 nM, 10 min; bars: 50 pA, 25 ms). Bar graph summarizes the results for prepubescent and adult female slices: L655,708 significantly increased the area of the burst response in adult ($n=12$; $P=0.003$, two-tailed paired *t*-test) but not prepubescent females ($n=13$; $P=0.144$). The difference in percentage increase above pre-drug baseline for the two groups was significant (two-tailed unpaired *t*-test: $^{*}P=0.04$). **d**, Adult female mice were intraperitoneally injected with vehicle (0.1% DMSO) or L655,708 (0.5 mg kg^{-1}) 30 min before the 5-min training trial for OLM. With a 24-h delay, adult females given L655,708 showed enhanced discrimination for the displaced object compared to vehicle-treated females (two-tailed unpaired *t*-test: $^{**}P=0.0097$; Vehicle: $n=8$ and L655,708: $n=7$). Mean ± s.e.m. values are shown. Statistics are summarized in Supplementary Table 1.

transmission activated by CA3 inputs to CA1 changes during female puberty. We accordingly counted the number of inhibitory synapses in the apical CA1 dendritic subfield evaluated in the physiological studies. Dual immunofluorescence for the post-synaptic scaffolding protein gephyrin and the pre-synaptic vesicular GABA transporter (VGAT) was used to label inhibitory synapses in female rats; three-dimensional (3D) reconstructions of several thousand individual pre-synaptic and post-synaptic elements were created from image *z*-stacks and quantified using fluorescence deconvolution tomography[38,39] (FDT) (Fig. 4a). There was no change in the incidence of inhibitory synapses (Fig. 4b) or the per-synapse density of gephyrin (Fig. 4c) or VGAT (not shown) immunoreactivity (-ir) from 4 to 8 weeks of age.

Next, we evaluated specific GABA$_A$R subunits co-localized with gephyrin beginning with the α5 subunit that has been linked to feed-forward inhibition in CA1[40]. Specifically, α5-GABA$_A$Rs are present in inhibitory synapses on CA1 pyramidal cell dendrites where they mediate slow decaying IPSCs. Deletion of α5 decreases the amplitude of spontaneous (synaptic) IPSCs in CA1 and increases paired-pulse facilitation of fEPSPs elicited by SC stimulation. The latter result constitutes evidence that a significant portion of feed-forward inhibition, which shunts the response to the second stimulation pulse, is mediated by α5-GABA$_A$Rs.

The α5 subunit levels at inhibitory (gephyrin-ir) synapses in CA1 stratum radiatum increased markedly from 4 to 8 weeks of age in females (Fig. 4d,e); this was evident as a right-shift in the immunolabeling density frequency distribution toward higher values in adults relative to juveniles ($F_{50,700}=14.46$, $P<0.0001$, repeated-measures ANOVA) (Fig. 4d, left). As expected from this, the percentage of synapses associated with high concentrations of α5-ir was more than two-fold greater after puberty (Fig. 4d, right). This developmental change was not present in males: the frequency distributions for densities of synaptic α5-ir were superimposable for prepubescent and adult groups ($F_{10,130}=0.46$, $P=0.91$) (Supplementary Fig. 2b), and the percentage of contacts with high concentrations of α5-ir was similar (pre-puberty: 20.6 ± 1.3%; post-puberty: 20.5 ± 2.2%) (Fig. 4d, right). Comparisons of males and females identified an interaction between sex and age ($F_{1,26}=15.30$, $P=0.0006$, two-way ANOVA). The density of synaptic α5-ir increased across female puberty ($P<0.0001$), and prepubescent males had higher levels than age-matched females ($P=0.033$). There were no differences between juvenile and adult males ($P=0.99$) or between adult males and females ($P=0.07$). In all, there was a striking difference between the sexes with regard to puberty-related changes in a key element of feed-forward GABAergic transmission in the CA1 apical dendritic field.

We analyzed two additional GABA$_A$R subunits to test the selectivity of the pre-puberty to post-puberty increase in α5 recorded for females. From 4 to 8 weeks of age, the density of immunoreactivity for the α2 subunit at gephyrin-ir synapses was unchanged ($F_{50,700}=0.17$, $P>0.99$, repeated-measures ANOVA) (Fig. 4f), and there was a slight shift toward higher densities of β1 subunit-ir, but this was not statistically significant ($F_{50,700}=1.32$, $P=0.07$) (Fig. 4g).

Effects of blocking α5-GABA$_A$Rs. We tested the prediction that blocking α5-GABA$_A$Rs with subunit-selective negative allosteric modulators (NAMs, also known as inverse agonists) would restore theta burst responses and LTP in adult female rats to levels found before puberty. Infusion of the selective α5-NAM L655,708 (150 nM, 40 min), which acts via the benzodiazepine binding site to suppress IPSCs gated by α5-GABA$_A$Rs, had minimal effects on baseline fEPSP amplitude in adult females but caused a clear enhancement of the normalized and raw amplitudes of the second–fourth potentials in the composite response to a theta burst, as expected for suppression of fast inhibition (Fig. 5a for normalized values; raw values: first pulse, vehicle: 2.75 ± 0.13 mV and L655,708: 3.00 ± 0.11 mV, two-tailed unpaired *t*-test: $P = 0.11$, repeated-measures ANOVA across pulses: $P = 0.0048$, $F_{3,39} = 5.041$). These results constitute the first evidence that α5-GABA$_A$Rs potently affect theta burst responses. We confirmed that theta burst triplets fail to elicit LTP in vehicle-treated adult female rat slices but do produce robust LTP in the presence of L655,708 (9.3 ± 2.9% versus 48.9 ± 6.7%; $P = 0.0002$, at 55–60 min after TBS, unpaired *t*-test) (Fig. 5b). Voltage-clamp recordings in mouse slices revealed that the NAM significantly increased (22.2 ± 4.8%; $P = 0.003$, paired *t*-test) the area of single theta burst responses above pre-treatment baseline in adult females. However, and in accordance with the analysis of α5 densities at synapses, the compound had little, if any, effect (8.3 ± 4.2%; $P = 0.144$) on response size in prepubescent female slices (prepubertal versus adult; $P = 0.04$, unpaired *t*-test) (Fig. 5c). Collectively, these findings indicate that the pronounced increase in synaptic α5-GABA$_A$Rs that occurs over the course of female puberty depresses theta burst responses, leading to an increase in LTP threshold.

As expected from the FDT analysis of synaptic α5 concentrations, L655,708 caused a similar increase in burst response area in males before and after puberty (area change: 26.6 ± 3.4% and 29.6 ± 4.7%, respectively; $P < 0.01$ within groups, paired *t*-tests; $P = 0.649$ between age groups, unpaired *t*-tests; Supplementary Fig. 2c).

Next, we tested the prediction that the recovery of low-threshold LTP in adult females produced by L655,708 would result in a similar improvement in spatial learning. Non-proestrus mice were injected with vehicle or the α5-NAM 30 min before 5-min OLM training and were tested for discrimination of the moved object 24 h later (Fig. 2a). Vehicle-treated mice had low retention scores, whereas the L655,708 group performed at the level of prepubescent females and adult males (vehicle versus L655,708: $P = 0.0097$, unpaired *t*-test) (Fig. 5d and Extended Data Fig. 2a). The NAM did not influence cue sampling times during training or testing or locomotor activity (Extended Data Fig. 2b,c,d).

Contributions of ERα to LTP before puberty. As described, LTP in adult females is dependent on locally synthesized estrogen acting on synaptic ERα[16]. We investigated the possibility that this requirement emerges with puberty, and associated increases in circulating estrogen[31], and, thus, is a potential contributor to the elevation of LTP thresholds. The selective ERα antagonist MPP produced a near complete blockade of potentiation induced by a train of ten theta bursts in slices from 4-week-old female rats (Vehicle: 58.9 ± 7.2% at 55–60 min after TBS and MPP: 12.4 ± 4.5%; $P = 0.0006$, unpaired *t*-test) (Fig. 6a). The use of a stronger induction paradigm (ten bursts instead of burst triplets) emphasizes the extent to which prepubescent female LTP is dependent on this estrogen receptor class. Using FDT, we determined that ERα levels at PSD-95-ir synapses in CA1 stratum radiatum are considerably higher in adult than prepubertal female rats ($F_{19,342} = 22.10$, $P < 0.0001$) (Fig. 6b). This result argues against a decline in ERα contributing to the age-related increase in LTP threshold. We previously showed that synaptic ERα levels are substantially higher in adult females than age-matched males[16], but this sex difference was not detected in prepubescent rats (Supplementary Fig. 2d,e). Moreover, synaptic concentrations of ERβ-ir in prepubertal and adult females were similar (Fig. 6c). Together, these findings raise the possibility that the marked and sex-specific change in synaptic ERα levels is a specialization that partially compensates for the reduction in the NMDAR component of the theta burst response that occurs in female rodents during the transition through puberty.

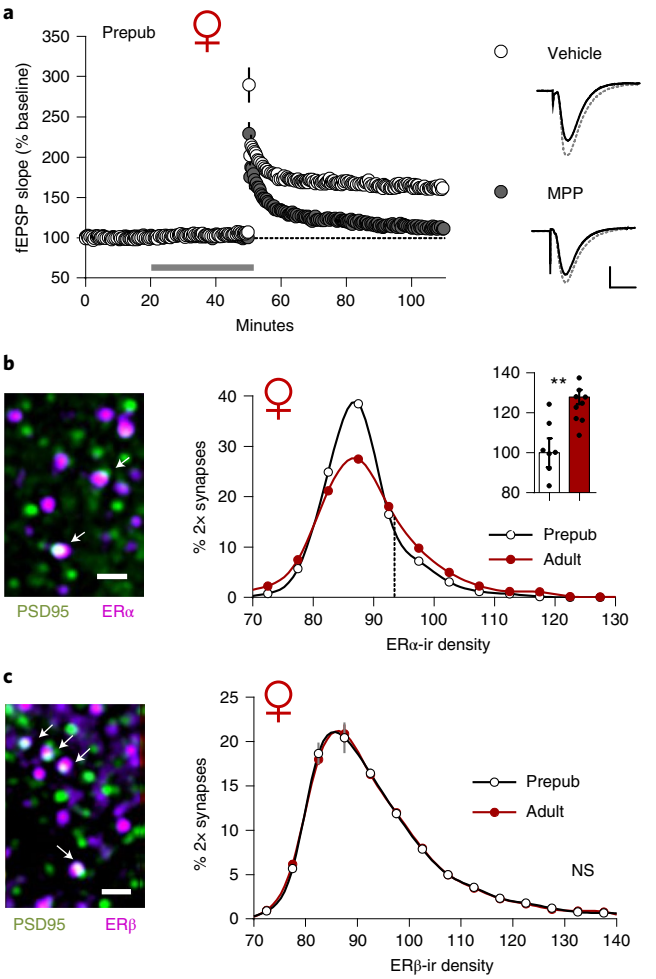

Fig. 6 | LTP induction in prepubescent female rats is dependent on activation of ERα. a, Slices from prepubertal female rats were infused for 30 min with ERα antagonist MPP or vehicle before SC stimulation with ten theta bursts. In the presence of MPP, LTP decayed to baseline within 1 h, whereas vehicle-treated cases exhibited robust and stable LTP (two-tailed unpaired *t*-test at 55–60 min after TBS: $P = 0.0006$; $n = 5$ per group). Traces (right) show superimposed pre-TBS (black) versus post-TBS (dashed) fEPSPs. Bars: 1 mV, 10 ms. **b**, Dual immunolabeling for ERα (magenta) and PSD-95 (green) in the CA1 lamina used for LTP experiments from prepubertal and adult females (deconvolved images; area of overlap (white) identified in 3D). Arrows highlight double-labeled contacts ('2× synapses'). The line graph summarizes the density frequency distributions for ERα-ir co-localized with PSD-95 as determined using FDT. Adult females show a significant rightward skew toward high densities relative to prepubescent animals (two-way repeated-measures ANOVA: $F_{19,342} = 22.10$, $P = 2.17 \times 10^{-48}$, $n = 10$ per group). The inset graph summarizes the percentage of higher-density contacts (92+ on *x* axis) (two-tailed unpaired *t*-test: $^{**}P = 0.002$ for pre-puberty versus post-puberty). **c**, Representative image of ERβ (magenta) and PSD-95 (green) double labeling. Synaptic ERβ density distribution curves were similar in prepubertal and adult females ($F_{19,323} = 0.16$, $P = 0.99$; Prepub: $n = 9$ and Adult: $n = 10$). Bar for **b**,**c**, 1 µm. Mean ± s.e.m. values are shown. Statistics are summarized in Supplementary Table 1. NS, not significant.

Discussion

The present results lead to the surprising conclusion that the polarity of sex differences at hippocampal synapses and related learning reverses from before to after puberty. This occurs because of opposite developmental changes in females versus males: thresholds for plasticity and encoding spatial information increase in females and decrease in males. We identified a plausible mechanism for the female effect: the depolarizing responses elicited by the short high-frequency stimulation bursts are substantially larger in the prepubertal animals. The bursts produce frequency facilitation of transmitter (glutamate) release at the SC synapses, but the expected enhancement of successive post-synaptic responses is partially shunted by the buildup of di-synaptic feed-forward IPSCs. The latter GABAergic responses are due to interneurons engaged by CA3-to-CA1 projections. Shunting is of considerable functional significance with regard to LTP because enhanced and prolonged depolarization is required to unblock the voltage-dependent, relatively slow NMDARs that initiate the complex sequences leading to synaptic modifications. We found that the shape of the composite response elicited by a four-pulse burst differed significantly between prepubescent and postpubescent females: responses to later pulses in the burst were larger in prepubertal animals, suggesting less inhibition at this age. Clamp recordings demonstrated that feed-forward inhibition during the bursts increases substantially at some point during female puberty.

The facilitation of responses that occurs when two bursts are given sequentially was also greater before than after female puberty. Previous work showed that the enhancement of the second response reflects a partial refractoriness of feed-forward inhibition due to $GABA_BR$ activation on interneuron terminals[41,42]. These metabotropic receptors open potassium channels and, thereby, reduce GABA release probability with the effect maximized at about the period of the theta wave. We interpret the greater facilitation of the second burst in prepubescent females as resulting from the refractory process operating on weaker inhibition. This effect is directly related to LTP threshold because the greater and temporally extended depolarization produced by the second burst suffices to open NMDAR channels. We confirmed that the NMDAR component of the second response is larger before than after puberty in females.

Despite age-related changes in activity-driven IPSCs, we did not detect an increase in the number or density of GABAergic contacts in CA1 stratum radiatum. This finding raised the possibility of developmental changes in the composition of $GABA_ARs$. The pentameric GABA receptors include one γ, two α and two β subunits[43]. The specific α subunits exert differential effects on rate kinetics. Receptors containing α5 are of particular interest in the present context because they generate large and prolonged IPSCs that shunt NMDAR-mediated currents in the apical dendrites of field CA1[44]. Notably, adult hippocampus in rodents and humans has unusually high levels of α5 expression[45–47]. Our analyses indicate that α5 levels at inhibitory synapses in apical field CA1 are substantially lower before puberty in females. The developmental difference in α5-$GABA_ARs$ in the same dendritic layer containing the excitatory SC synapses that generate the theta burst response helps explain why later potentials in those responses are unusually large in prepubescent females. In accordance with the above arguments, we found that negative modulation of α5-$GABA_ARs$ restored theta burst responses, LTP thresholds and spatial learning in adult females to levels found before puberty.

The changes in α5 concentrations could reflect the developmental onset of the estrous cycle, which occurs around P28–30 depending on rodent strain and species[31], as multiple studies have shown that this influences the $GABA_AR$ subunit composition[48–51]. These effects have been related to fluctuations in progesterone and its neurosteroid metabolites[49]. The steroids operate over different time courses and mechanisms, including effects on $GABA_AR$ subunit gene expression[50,51]. These analyses have only recently extended to α5 in rodents[52] and, as yet, do not provide an interpretation for the present findings. An alternative possibility involves the late maturation of interneurons and their connections. Neuronal activity affects expression of cell-specific transcription factors, including Npas4, that influence the formation of excitatory synapses on somatostatin-positive interneurons[53,54]. Relatedly, network activity influences elements of perineuronal nets associated with parvalbumin-positive interneurons, a specialization widely held to alter synaptic connectivity[53,55]. There is also evidence that activity influences the expression of channels by parvalbumin interneurons, including the potassium and voltage-gated Kv1.1, that regulate the excitability and firing characteristics of these cells[56,57]. It is, thus, possible that the change from prepubertal to postpubertal life is associated with changes in interneuron function that alter post-synaptic cells in a manner that shifts the balance of inhibitory synapses in favor of those enriched with α5-$GABA_ARs$.

The absence of age-related changes in the density of α5-ir at inhibitory synapses in males constitutes one of the more striking sex differences observed in the present studies. It is clear from this, and related observations, that changes in shunting IPSCs and theta burst responses are not responsible for the emergence of low-threshold LTP in postpubertal males. In males, burst responses were, if anything, reduced from before to after puberty, which strongly suggests that NMDAR-gated ionic currents did not increase. There remains the possibility that calcium influx through the receptors, or the subsequent release of the cation from intracellular stores, increases from 4 to 8 weeks of age in males. Alternatively, recent studies raise the possibility that NMDAR-mediated activation of the LTP critical kinase Src involves non-ionic functions; a metabotropic route is also suggested for NMDAR-dependent ERK activation[58,59]. A change in the linkages between the NMDARs and these enzymes during puberty could account for the observed drop in male LTP threshold.

Given the extensive evidence linking LTP to some, but not all, forms of learning, an increase in the threshold for inducing LTP is likely to have considerable consequences for behavior. In accordance with this, postpubescent females did not acquire simple or complex spatial information with a minimal number of trials, tests on which excellent scores were observed before puberty. Notably, pharmacological suppression of α5-$GABA_ARs$ restored LTP and memory encoding in adult females to levels observed before puberty. One interpretation of the seemingly deleterious elevation of plasticity and learning thresholds is that the effects are secondary to adaptations for other, unrelated female behaviors. The α5-containing $GABA_ARs$ have been linked to anxiety[60–62], a psychological variable that can be strongly affected in a sex-specific manner by puberty[63–65]. Possibly, then, an adaptation involving emotional behaviors appropriate to the transition to early adult life affects learning mechanisms as a side effect. Moreover, slower encoding could have advantages in complex real-world environments that contain multiple cues and choices, circumstances in which it is necessary to distinguish reliable signals from noise. If so, then adaptive pressures relating to typical mammalian sex differences in the variety and extent of social roles, including extremely complex care of altricial offspring, might have resulted in opposing late developmental adjustments to learning mechanisms.

Finally, evidence that hippocampal LTP threshold changes in opposite directions, between males and females, in the transition to postpubertal life raises the question of whether there are similar effects in other brain regions. This issue has yet to be addressed, but there is reason to expect that the hippocampal changes influence broader network function. The hippocampus works in concert with parahippocampal and medial prefrontal cortex[66], and cooperativity with the latter is reportedly critical for realizing estrogen effects on encoding spatial and episodic memory[67,68]. This suggests that

hippocampal changes described here likely influence functions of the larger hippocampal–prefrontal cortical system, including behaviors ascribed to the cortical field.

Online content

Any methods, additional references, Nature Research reporting summaries, source data, extended data, supplementary information, acknowledgements, peer review information; details of author contributions and competing interests; and statements of data and code availability are available at https://doi.org/10.1038/s41593-021-01001-5.

Received: 19 March 2021; Accepted: 9 December 2021;
Published online: 27 January 2022

References

1. Andreano, J. M. & Cahill, L. Sex influences on the neurobiology of learning and memory. *Learn. Mem.* **16**, 248–266 (2009).
2. Koss, W. A. & Frick, K. M. Sex differences in hippocampal function. *J. Neurosci. Res.* **95**, 539–562 (2017).
3. Tascón, L. et al. Sex differences in spatial memory: comparison of three tasks using the same virtual context. *Brain Sci.* **11**, 757 (2021).
4. Bocchi, A. et al. The role of gender and familiarity in a modified version of the almeria boxes room spatial task. *Brain Sci.* **11**, 681 (2021).
5. Voyer, D., Voyer, S. D. & Saint-Aubin, J. Sex differences in visual-spatial working memory: a meta-analysis. *Psychon. Bull. Rev.* **24**, 307–334 (2017).
6. Voyer, D., Voyer, S. & Bryden, M. P. Magnitude of sex differences in spatial abilities: a meta-analysis and consideration of critical variables. *Psychol. Bull.* **117**, 250–270 (1995).
7. Seurinck, R., Vingerhoets, G., de Lange, F. P. & Achten, E. Does egocentric mental rotation elicit sex differences? *Neuroimage* **23**, 1440–1449 (2004).
8. Yagi, S. & Galea, L. A. M. Sex differences in hippocampal cognition and neurogenesis. *Neuropsychopharmacology* **44**, 200–213 (2019).
9. Jones, C. M., Braithwaite, V. A. & Healy, S. D. The evolution of sex differences in spatial ability. *Behav. Neurosci.* **117**, 403–411 (2003).
10. Vierk, R. et al. Aromatase inhibition abolishes LTP generation in female but not in male mice. *J. Neurosci.* **32**, 8116–8126 (2012).
11. Hojo, Y. et al. Adult male rat hippocampus synthesizes estradiol from pregnenolone by cytochromes P45017α and P450 aromatase localized in neurons. *Proc. Natl Acad. Sci. USA* **101**, 865–870 (2004).
12. Kato, A. et al. Female hippocampal estrogens have a significant correlation with cyclic fluctuation of hippocampal spines. *Front. Neural Circuits* **7**, 149 (2013).
13. Tabatadze, N., Sato, S. M. & Woolley, C. S. Quantitative analysis of long-form aromatase mRNA in the male and female rat brain. *PLoS ONE* **9**, e100628 (2014).
14. Mukai, H. et al. Modulation of synaptic plasticity by brain estrogen in the hippocampus. *Biochim. Biophys. Acta* **1800**, 1030–1044 (2010).
15. Ooishi, Y. et al. Modulation of synaptic plasticity in the hippocampus by hippocampus-derived estrogen and androgen. *J. Steroid Biochem. Mol. Biol.* **131**, 37–51 (2012).
16. Wang, W. et al. Memory-related synaptic plasticity is sexually dimorphic in rodent hippocampus. *J. Neurosci.* **38**, 7935–7951 (2018).
17. Kight, K. E. & McCarthy, M. M. Androgens and the developing hippocampus. *Biol. Sex. Differ.* **11**, 30 (2020).
18. Juraska, J. M. & Willing, J. Pubertal onset as a critical transition for neural development and cognition. *Brain Res.* **1654**, 87–94 (2017).
19. Sisk, C. L. & Zehr, J. L. Pubertal hormones organize the adolescent brain and behavior. *Front. Neuroendocrinol.* **26**, 163–174 (2005).
20. Baudry, M., Arst, D., Oliver, M. & Lynch, G. Development of glutamate binding sites and their regulation by calcium in rat hippocampus. *Brain Res.* **227**, 37–48 (1981).
21. Muller, D., Oliver, M. & Lynch, G. Developmental changes in synaptic properties in hippocampus of neonatal rats. *Brain Res. Dev. Brain Res.* **49**, 105–114 (1989).
22. Figurov, A., Pozzo-Miller, L. D., Olafsson, P., Wang, T. & Lu, B. Regulation of synaptic responses to high-frequency stimulation and LTP by neurotrophins in the hippocampus. *Nature* **381**, 706–709 (1996).
23. Shen, H. et al. A critical role for α4βδ $GABA_A$ receptors in shaping learning deficits at puberty in mice. *Science* **327**, 1515–1518 (2010).
24. Smith, S. S. The influence of stress at puberty on mood and learning: role of the α4βδ $GABA_A$ receptor. *Neuroscience* **249**, 192–213 (2013).
25. Pattwell, S. S., Lee, F. S. & Casey, B. J. Fear learning and memory across adolescent development: hormones and behavior special issue: puberty and adolescence. *Horm. Behav.* **64**, 380–389 (2013).
26. Romeo, R. D. Puberty: a period of both organizational and activational effects of steroid hormones on neurobehavioural development. *J. Neuroendocrinol.* **15**, 1185–1192 (2003).
27. Larson, J. & Lynch, G. Induction of synaptic potentiation in hippocampus by patterned stimulation involves two events. *Science* **232**, 985–988 (1986).
28. Barrett, R. M. et al. Hippocampal focal knockout of CBP affects specific histone modifications, long-term potentiation, and long-term memory. *Neuropsychopharmacology* **36**, 1545–1556 (2011).
29. Inagaki, T., Gautreaux, C. & Luine, V. Acute estrogen treatment facilitates recognition memory consolidation and alters monoamine levels in memory-related brain areas. *Horm. Behav.* **58**, 415–426 (2010).
30. Boulware, M. I., Heisler, J. D. & Frick, K. M. The memory-enhancing effects of hippocampal estrogen receptor activation involve metabotropic glutamate receptor signaling. *J. Neurosci.* **33**, 15184–15194 (2013).
31. Bell, M. R. Comparing postnatal development of gonadal hormones and associated social behaviors in rats, mice, and humans. *Endocrinology* **159**, 2596–2613 (2018).
32. Alger, B. E. & Nicoll, R. A. Feed-forward dendritic inhibition in rat hippocampal pyramidal cells studied in vitro. *J. Physiol.* **328**, 105–123 (1982).
33. Larson, J. & Munkácsy, E. Theta-burst LTP. *Brain Res.* **1621**, 38–50 (2015).
34. Ben-Ari, Y., Krnjević, K., Reiffenstein, R. J. & Reinhardt, W. Inhibitory conductance changes and action of γ-aminobutyrate in rat hippocampus. *Neuroscience* **6**, 2445–2463 (1981).
35. Pacelli, G. J., Su, W. & Kelso, S. R. Activity-induced decrease in early and late inhibitory synaptic conductances in hippocampus. *Synapse* **7**, 1–13 (1991).
36. Pacelli, G. J., Su, W. & Kelso, S. R. Activity-induced depression of synaptic inhibition during LTP-inducing patterned stimulation. *Brain Res.* **486**, 26–32 (1989).
37. Larson, J. & Lynch, G. Role of *N*-methyl-D-aspartate receptors in the induction of synaptic potentiation by burst stimulation patterned after the hippocampal θ-rhythm. *Brain Res.* **441**, 111–118 (1988).
38. Rex, C. S. et al. Different Rho GTPase-dependent signaling pathways initiate sequential steps in the consolidation of long-term potentiation. *J. Cell Biol.* **186**, 85–97 (2009).
39. Seese, R. R. et al. Synaptic abnormalities in the infralimbic cortex of a model of congenital depression. *J. Neurosci.* **33**, 13441–13448 (2013).
40. Schulz, J. M., Knoflach, F., Hernandez, M. C. & Bischofberger, J. Dendrite-targeting interneurons control synaptic NMDA-receptor activation via nonlinear α5-GABA. *Nat. Commun.* **9**, 3576 (2018).
41. Davies, C. H., Starkey, S. J., Pozza, M. F. & Collingridge, G. L. GABA autoreceptors regulate the induction of LTP. *Nature* **349**, 609–611 (1991).
42. Mott, D. D. & Lewis, D. V. Facilitation of the induction of long-term potentiation by $GABA_B$ receptors. *Science* **252**, 1718–1720 (1991).
43. Sigel, E. & Steinmann, M. E. Structure, function, and modulation of $GABA_A$ receptors. *J. Biol. Chem.* **287**, 40224–40231 (2012).
44. Collinson, N. et al. Enhanced learning and memory and altered GABAergic synaptic transmission in mice lacking the α5 subunit of the $GABA_A$ receptor. *J. Neurosci.* **22**, 5572–5580 (2002).
45. Sieghart, W. & Sperk, G. Subunit composition, distribution and function of $GABA_A$ receptor subtypes. *Curr. Top. Med. Chem.* **2**, 795–816 (2002).
46. Sur, C., Quirk, K., Dewar, D., Atack, J. & McKernan, R. Rat and human hippocampal α5 subunit-containing γ-aminobutyric $Acid_A$ receptors have α5β3γ2 pharmacological characteristics. *Mol. Pharmacol.* **54**, 928–933 (1998).
47. Wainwright, A., Sirinathsinghji, D. J. & Oliver, K. R. Expression of $GABA_A$ receptor α5 subunit-like immunoreactivity in human hippocampus. *Brain Res. Mol. Brain Res.* **80**, 228–232 (2000).
48. Mukherjee, J. et al. Estradiol modulates the efficacy of synaptic inhibition by decreasing the dwell time of GABA. *Proc. Natl Acad. Sci. USA* **114**, 11763–11768 (2017).
49. Weiland, N. G. & Orchinik, M. Specific subunit mRNAs of the $GABA_A$ receptor are regulated by progesterone in subfields of the hippocampus. *Brain Res. Mol. Brain Res.* **32**, 271–278 (1995).
50. Herbison, A. E. & Fénelon, V. S. Estrogen regulation of $GABA_A$ receptor subunit mRNA expression in preoptic area and bed nucleus of the stria terminalis of female rat brain. *J. Neurosci.* **15**, 2328–2337 (1995).
51. Vastagh, C., Rodolosse, A., Solymosi, N. & Liposits, Z. Altered expression of genes encoding neurotransmitter receptors in GnRH neurons of proestrous mice. *Front. Cell Neurosci.* **10**, 230 (2016).
52. Franco-Enzástiga, Ú. et al. Sex-dependent pronociceptive role of spinal α_5-$GABA_A$ receptor and its epigenetic regulation in neuropathic rodents *J. Neurochem.* **156**, 897–916 (2021).
53. Spiegel, I. et al. Npas4 regulates excitatory-inhibitory balance within neural circuits through cell-type-specific gene programs. *Cell* **157**, 1216–1229 (2014).
54. Sim, S. et al. Increased cell-intrinsic excitability induces synaptic changes in new neurons in the adult dentate gyrus that require Npas4. *J. Neurosci.* **33**, 7928–7940 (2013).

55. Shepard, R., Heslin, K., Hagerdorn, P. & Coutellier, L. Downregulation of Npas4 in parvalbumin interneurons and cognitive deficits after neonatal NMDA receptor blockade: relevance for schizophrenia. *Transl. Psychiatry* **9**, 99 (2019).
56. Morgan, P. J., Bourboulou, R., Filippi, C., Koenig-Gambini, J. & Epsztein, J. Kv1.1 contributes to a rapid homeostatic plasticity of intrinsic excitability in CA1 pyramidal neurons in vivo. *eLife* **8**, e49915 (2019).
57. Monaghan, M. M., Trimmer, J. S. & Rhodes, K. J. Experimental localization of Kv1 family voltage-gated K^+ channel α and β subunits in rat hippocampal formation. *J. Neurosci.* **21**, 5973–5983 (2001).
58. Dore, K., Aow, J. & Malinow, R. The emergence of NMDA receptor metabotropic function: insights from imaging. *Front. Synaptic Neurosci.* **8**, 20 (2016).
59. Nabavi, S. et al. Metabotropic NMDA receptor function is required for NMDA receptor-dependent long-term depression. *Proc. Natl Acad. Sci. USA* **110**, 4027–4032 (2013).
60. Clayton, T. et al. A review of the updated pharmacophore for the α5 $GABA_A$ benzodiazepine receptor model. *Int J. Med. Chem.* **2015**, 430248 (2015).
61. Navarro, J. F., Burón, E. & Martín-López, M. Anxiogenic-like activity of L-655,708, a selective ligand for the benzodiazepine site of $GABA_A$ receptors which contain the alpha-5 subunit, in the elevated plus-maze test. *Prog. Neuropsychopharmacol. Biol. Psychiatry* **26**, 1389–1392 (2002).
62. Magnin, E. et al. Input-specific synaptic location and function of the α5 GABA. *J. Neurosci.* **39**, 788–801 (2019).
63. Costello, E. J., Copeland, W. & Angold, A. Trends in psychopathology across the adolescent years: what changes when children become adolescents, and when adolescents become adults? *J. Child Psychol. Psychiatry* **52**, 1015–1025 (2011).
64. Asher, M., Asnaani, A. & Aderka, I. M. Gender differences in social anxiety disorder: a review. *Clin. Psychol. Rev.* **56**, 1–12 (2017).
65. Altemus, M., Sarvaiya, N. & Neill Epperson, C. Sex differences in anxiety and depression clinical perspectives. *Front. Neuroendocrinol.* **35**, 320–330 (2014).
66. Eichenbaum, H. Prefrontal–hippocampal interactions in episodic memory. *Nat. Rev. Neurosci.* **18**, 547–558 (2017).
67. Schwabe, M. R., Taxier, L. R. & Frick, K. M. It takes a neural village: circuit-based approaches for estrogenic regulation of episodic memory. *Front. Neuroendocrinol.* **59**, 100860 (2020).
68. Tuscher, J. J., Taxier, L. R., Schalk, J. C., Haertel, J. M. & Frick, K. M. Chemogenetic suppression of medial prefrontal-dorsal hippocampal interactions prevents estrogenic enhancement of memory consolidation in female mice. *eNeuro* **6**, ENEURO.0451-18.2019 (2019).

Methods

Animals. The studies used P21–26 and 2–4-month-old male and female mice (FVB129 background) and P21–28 and 2–3-month-old Sprague Dawley male and female rats. We used rats for most of the electrophysiological experiments (excepting the use of mice for analysis in Fig. 5c) and all of the immunolabeling experiments because their larger hippocampus allowed for greater precision in aligning zones used in the imaging methods with those sampled during recording studies. Mice were used in all behavior experiments to allow for larger sample size and because tasks have been validated in mice. Animals were on a 12-h light/dark cycle with lights on at 6:30AM and food and water ad libitum. Mice were grouped by 3–5 littermates and rats by 2–4 littermates per cage in rooms maintained at 68 °F and 55% humidity. Experiments were conducted in accordance with the National Institutes of Health Guide for the Care and Use of Laboratory Animals and protocols approved by the Institutional Animal Care and Use Committee at the University of California, Irvine. All adult females were estrous staged using vaginal lavage as described[69,70] and identified as proestrus (presence of nucleated cells) and non-proestrus (cornified cells for estrus stage and leukocytes for metestrus/diestrus). Prepubescent females were defined as P21–26 in mice and P21–P28 in rats to reflect differences in puberty onset, as defined visually by vaginal canal opening in both species[31]. Prepubescent male rats and mice were age-matched to conspecific females.

OLM (also known as object placement). Behavioral experiments were performed as described[16,71] in FVB129 mice. Animals were handled for 2 min per day for 2 d and then habituated to an empty arena (30 cm × 25 cm floor, 21.5-cm walls) for 5 min on each of the subsequent 4 d. For training, mice were returned to the arena containing two identical glass funnels that were 1 cm away from two adjacent corners; they were allowed to explore for 5 or 10 min; and then they were returned to their home cage. After a specified time delay, the mice were placed in the same arena with one funnel displaced toward the center and allowed to explore for 5 min.

Adult female mice were monitored for estrous cycling for at least 7 d before the training day to ensure normal cycling. On the training day, animals were separated into proestrus versus non-proestrus (estrus, metaestrus and diestrus were pooled) groups[12]. Prepubescent mice were P25 at training and did not show evidence of vaginal opening on training or testing days. For studies with L655,708, adult female mice were randomly assigned to the drug or vehicle group on the training day.

For these and other behavioral paradigms, animal movements within the test chamber were recorded by overhead camera during both training and testing. Videos were hand-scored by observers blinded to the group, and sampling time was recorded when the animal's nose sniffed the object within 0.5 cm. Sampling was not noted if the animal's nose was in the same zone while turning its head but not attending to the object. The DI was calculated by $100 \times (t_{\text{novel object}} - t_{\text{familiar object}})/(t_{\text{novel object}} + t_{\text{familiar object}})$.

Episodic 'Where' task. Studies used FVB129 mice as previously described[72]. The mice were handled 1 d before the task. On training day, the mice were then placed into a plexiglas arena (60 cm × 60 cm floor, 30-cm walls) containing four empty glass cups (5.25 cm in diameter × 5 cm in height) with a metal lid with a single hole (~1.5 cm in diameter). The cups were removed from the chamber, and the animal rested undisturbed for 5 min. For the training session, the four cups were re-introduced with each containing one of the following odorants dissolved in mineral oil (final concentration of 0.1 Pascals): (A) (+)-Limonene (≥97% purity, Sigma-Aldrich), (B) Cyclohexyl ethyl acetate (≥97%, International Flavors & Fragrances), (C) (+)-Citronellal (~96% Alfa Aesar) and (D) Octyl Aldehyde (~99%, Acros Organics). The animals' behavior was monitored over 5 min of odor exposure, and then they were returned to their home cage for 24 h. For testing, the animals were allowed to explore the chamber with either odorant pairs (A:D or B:C) switched in position for 5 min.

Episodic 'What' Task. The task followed the same setup as in the episodic 'Where' task, but, for training, the animals were exposed to odorant B, C, D and E (Anisole, ~99%, Acros Organics) for 5 min. The next day, the animals returned to the chamber with odorant A replacing odorants B or D and were allowed to explore the arena for 5 min.

For episodic 'Where' and 'What' tasks, video recordings of behavior were hand-scored by observers who were blinded to odors and groups. Cue sampling time was designated as the time the animal's nose was oriented toward the odor hole and within a 0.5-cm radius. The DI for the 'Where' task was calculated as follows: $100 \times (t_{\text{sum of switched pair}} - t_{\text{sum of stationary pair}})/(t_{\text{total sampling}})$. For the 'What' task, DI was calculated as follows: $100 \times (t_{\text{novel}} - t_{\text{mean familiars}})/(t_{\text{total sampling}})$.

Extracellular hippocampal slice recording. Transverse rat hippocampal slices (370 µm thick) were prepared using the McIllwain chopper and then transferred to an interface recording chamber, with constant oxygenated artificial cerebrospinal fluid (aCSF) perfusion (60–70 ml h^{-1}, 31 ± 1 °C) as described[16]. The aCSF was composed of (in mM): 124 NaCl, 26 $NaHCO_3$, 3 KCl, 1.25 KH_2PO_4, 2.5 $CaCl_2$, 1.5 $MgSO_4$ and 10 dextrose (pH 7.4, 300–310 mOsm). Recordings started 1.5–2 h after slice preparation. Field EPSPs were elicited using a twisted nichrome wire stimulating electrode and recorded with glass pipette electrode (2 M NaCl, R = 2–3 MΩ). These electrodes were placed in dorsal CA1b stratum radiatum equidistant from the CA1 stratum pyramidale. Single-pulse baseline stimulation was applied at 0.05 Hz with baseline intensity set to 50–60% of the maximum population spike-free fEPSP amplitude. All recordings were digitized at 20 kHz using an AC amplifier (A-M Systems, Model 1700), and sweeps of 1.5-s duration were recorded every 20 s using NAC 2.0 Neurodata Acquisition System (Theta Burst Corporation). After baseline recording and additional drug infusion, LTP was induced by applying ten bursts of TBS (four bursts at 100 Hz with a 200-ms interval between bursts) or threshold TBS (four triplets of theta bursts with a 200-ms interval between bursts within the triplet and 90 s between triplets), and the recording to baseline (0.05 Hz) stimulation resumed for 1 h. Female rat vaginal smears for estrous monitoring were collected postmortem at the time of slice preparation, and only non-proestrus animals were included in LTP experiments. Experiments using APV included all stages as there were no statistical differences between proestrus and non-proestrus stages. For all electrophysiology experiments, multiple slices from at least four rats were used, and the *n* reported was the number of slices.

Whole-cell voltage current-clamp recording. Hippocampal slices were prepared on the horizontal plane at a thickness of 350 µm from 4-week-old and 8-week-old mice and rats using a Leica vibrating tissue slicer (VT1000S). Slices were placed in a submerged recording chamber and continuously perfused at 2 ml min^{-1} with oxygenated (95% O_2/5% CO_2) aCSF at 32 °C. Whole-cell recordings (Axopatch 200 A amplifier, Molecular Devices) were made with 4–7-MΩ recording pipettes filled with a solution containing (in mM): 140 $CsMeSO_3$, 8 CsCl, 10 HEPES, 0.2 EGTA, 2 QX-314, 2 Mg-ATP and 0.3 Na-GTP. Osmolarity was adjusted to 290–295 mOsm and pH 7.4. Bipolar stimulating electrodes were placed in CA1 stratum radiatum, 100–150 µm from the recording cell. EPSCs were recorded by clamping the pyramidal cell at −50 mV in the presence of 50 µM APV. Data were collected using Clampex 10.6 and analyzed with Clampfit 10.6 (Molecular Devices).

Drug application. For hippocampal slice recording, the compounds were infused into the aCSF bath via an independent perfusion line (6 ml h^{-1}). Final aCSF bath concentrations: APV (100 µM; Hello Bio, HB0225), bicuculline (20 µM; Tocris Bioscience, 0130), L655,708 (field electrophysiology: 150 nM, whole-cell electrophysiology: 50 nM; Tocris Bioscience, 1327) and MPP dihydrochloride (3 µM; Tocris Bioscience, 1991) were dissolved in DMSO (<0.01%). For the OLM task, vehicle (0.1% DMSO) or L655,708 (0.5 mg kg^{-1} in 0.1% DMSO) was injected intraperitoneally 30 min before training.

FDT. Prepubescent female and male rats were sacrificed on P25; all adult female rats were sacrificed during the diestrus stage of the estrous cycle (P57–59), and adult male rats were age-matched. Slide-mounted, fresh-frozen tissue sections (25 µm, coronal) from mid-septotemporal hippocampus (same region used for electrophysiological studies) were immersion-fixed in 4% paraformaldehyde and processed for dual immunofluorescence as previously described[38,39,71,73] with incubation in primary antisera at 4 °C for 24 h and in secondary antisera at room temperature for 2 h. After the secondary incubation, sections were washed in 0.1 M phosphate buffer and cover-slipped using VectaShield with DAPI (Vector Labs).

Primary antisera cocktails included rabbit anti-gephyrin (1:2,000; Abcam, ab32206; RRID: AB_1860490) combined with either guinea pig anti-β1-$GABA_AR$ (1:500; Synaptic Systems, 224705; RRID: AB_2619940) or mouse anti-α2-$GABA_AR$ (1:500; Abcam, ab193311; RRID: AB_2890213); mouse anti-gephyrin (1:1,500; Synaptic Systems, 147021; RRID: AB_2232546) combined with either guinea pig anti-vGAT (1:2,000; Synaptic Systems, 131004; RRID: AB_887873) or rabbit anti-α5-$GABA_AR$ (1:800; Abcam, ab10098; RRID: AB_296840); rabbit anti-ERα (1:700; Santa Cruz Biotechnology, sc-542; RRID: AB_631470) combined with mouse anti-PSD-95 (1:1,000; Thermo Fisher Scientific, MA1-045; RRID: AB_325399); and mouse anti-ERβ (1:700; Santa Cruz Biotechnology, sc-390243; RRID: AB_2728765) combined with goat anti-PSD-95 (1:1,000; Abcam, ab12093; RRID: AB_298846). Secondary antibodies (all at 1:1,000 dilution) included donkey anti-rabbit Alexa Fluor 594 (Invitrogen, Thermo Fisher Scientific, A-21207; RRID: AB_141637), goat anti-guinea pig Alexa Fluor 488 (Invitrogen, Thermo Fisher Scientific, A-11073; RRID: AB_2534117), donkey anti-goat Alexa Fluor 488 (Invitrogen, Thermo Fisher Scientific, A-11055; RRID: AB_2534102) and donkey anti-mouse Alexa Fluor 488 (Invitrogen, Thermo Fisher Scientific, A-21202; RRID: AB_141607).

FDT was conducted as described[16,38,71,73]. Under ×63 magnification, image *z*-stacks (136 × 105 × 2 µm) were collected using 200-nm steps from CA1 stratum radiatum; for each case, images were collected from five or more sections spaced by 250 µm on the septotemporal axis of hippocampus. The images were processed for iterative deconvolution (99% confidence; Volocity 4.0). Individual stacks were used to construct 3D montages of each sample field. Labeled objects were detected using threshold image segmentation across each channel separately. An image was normalized and thresholded at a given intensity threshold; erosion and dilation were used to fill holes and remove background pixels; and objects were segmented based on connected pixels above a threshold using in-house software (using C99, Java (OpenJDK IcedTea 6.1.12.6), MATLAB R2019b, PuTTY 0.74 and Perl version 5.30.0). All immunofluorescent elements meeting size constraints of synapses and detected across multiple intensity thresholds were quantified using automated

systems. The gephyrin and PSD-95-immunoreactive elements were considered to be double-labeled for the second antigen if there was contact or overlap in fields of the two fluorophores as assessed in 3D. Using this approach, ~30,000 inhibitory or excitatory synapses were reconstructed per sample field, and more than 150,000 were analyzed per rat.

Statistics. Results are presented as mean ± s.e.m. For LTP studies, significance was determined by comparing the within-slice normalized mean response over the last 5 min of the experiment between groups using two-tailed unpaired *t*-test or two-way ANOVA with post hoc Tukey test. Significance in STP and burst pulse analyses was determined using repeated-measures ANOVA with Bonferroni post hoc test. Whole-cell recordings and input–output curves were analyzed using two-tailed unpaired and paired *t*-tests and linear regression, respectively. Behavioral data were analyzed with two-way ANOVA with post hoc Tukey test for age and sex comparisons or unpaired or paired two-tailed Student *t*-test for two-group comparisons. For FDT density frequency distributions, significance was determined using two-way repeated-measures ANOVA. For statistical comparison of mean data between two groups, Student *t*-test was used. For age and sex comparisons, two-way ANOVA was used followed by post hoc Tukey test. All analyses were performed using Prism 6.0 (GraphPad).

Reporting Summary. Further information on research design is available in the Nature Research Reporting Summary linked to this article.

Data availability

The data that support the findings of this study are available in this manuscript and the Supplementary Information. Source data are provided with this paper.

Code availability

Single and theta burst parameters for field electrophysiology were analyzed using code available at https://github.com/cdcox/Theta-burst-analyzer-for-Le-et-al. Code for FDT analysis is available upon reasonable request. The use of the FDT code is strictly prohibited without a licensing agreement from the University of California, Irvine.

References

69. Caligioni, C. S. Assessing reproductive status/stages in mice. *Curr. Protoc. Neurosci.* **48**, A.4I.1–A.4I.8 (2009).
70. Cora, M. C., Kooistra, L. & Travlos, G. Vaginal cytology of the laboratory rat and mouse: review and criteria for the staging of the estrous cycle using stained vaginal smears. *Toxicol. Pathol.* **43**, 776–793 (2015).
71. Seese, R. R., Wang, K., Yao, Y. Q., Lynch, G. & Gall, C. M. Spaced training rescues memory and ERK1/2 signaling in fragile X syndrome model mice. *Proc. Natl Acad. Sci. USA* **111**, 16907–16912 (2014).
72. Cox, B. M. et al. Acquisition of temporal order requires an intact CA3 commissural/associational (C/A) feedback system in mice. *Commun. Biol.* **2**, 251 (2019).
73. Babayan, A. H. et al. Integrin dynamics produce a delayed stage of long-term potentiation and memory consolidation. *J. Neurosci.* **32**, 12854–12861 (2012).

Acknowledgements

The authors thank E. Tran and G. Zalaya for assistance with behavioral studies. A.A.L. was supported by National Institute of Mental Health training grant T32-MH119049-02. J.C.L., Y.J., W.W., C.M.G. and G.L. were supported by Eunice Kennedy Shriver National Institute of Child Health and Human Development grant HD-089491, and G.L. was supported by National Science Foundation grant BCS-1941216. J.C.L., C.M.G. and G.L. were supported by National Institute on Drug Abuse grant DA-044118. G.L. and C.D.C. were supported by Office of Naval Research grant N00014182114, and C.D.C. was also supported by National Institutues of Health grant T32 AG00096-34.

Author contributions

A.A.L., C.M.G., G.L. and J.C.L. wrote the manuscript and designed experiments. A.A.L., J.C.L., Y.J. and W.W. performed experiments. C.D.C. constructed computerized analyses for the imaging and electrophysiological experiments.

Competing interests

The authors declare no competing interests.

Additional information

Extended data is available for this paper at https://doi.org/10.1038/s41593-021-01001-5.

Supplementary information The online version contains supplementary material available at https://doi.org/10.1038/s41593-021-01001-5.

Correspondence and requests for materials should be addressed to Christine M. Gall or Gary Lynch.

Peer review information *Nature Neuroscience* thanks Paul Frankland, Natalie Tronson, and the other, anonymous, reviewer(s) for their contribution to the peer review of this work.

Reprints and permissions information is available at www.nature.com/reprints.

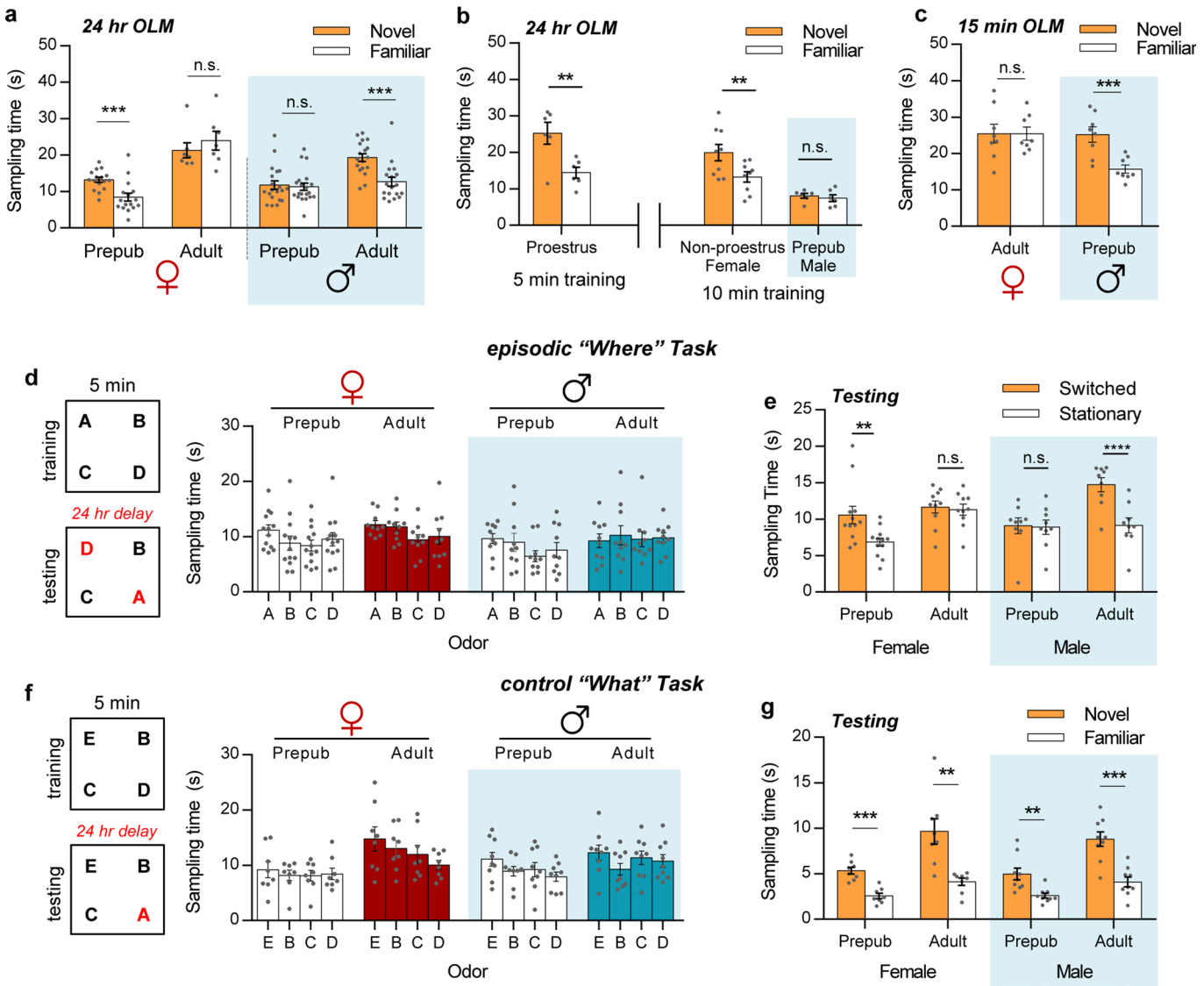

Extended Data Fig. 1 | Sampling times for each cue in Object Location Memory (OLM), 'Where', and 'What' tasks across age and sex. (**a**) OLM (5-min training session, tested 24 hours later): Sampling times of displaced (Novel) vs the stationary (Familiar) objects were compared for male and female mice of prepubescent (Prepub) and adult ages. Prepubescent females and adult males preferentially sampled the displaced object (***P = 0.0001, ***P = 0.0006, respectively; 2-tailed paired t-test), whereas non-proestrus adult females and prepubescent males did not (n.s. P = 0.21, P = 0.73, respectively; N = 7-18/group). (**b**) OLM (5- or 10-min training, tested 24-hours later): Adult females trained for 5 minutes during proestrus stage preferentially sampled the displaced object over the stationary object (**P = 0.004). Non-proestrus adult females and prepubescent males were trained for 10 minutes. Non-proestrus females preferred the displaced object (**P = 0.01), but the prepubescent males did not (n.s. P = 0.46; N = 6-9/group). (**c**) OLM (5-min training, 15-min delay): Adult females did not spend more time with the moved object (P = 0.99), whereas Prepub males preferred the moved object (***P = 0.0002; N = 8/group). (**d**) *Left*. Schematic for episodic 'Where' task with four odors (see Methods). *Right*. Sampling times of odors A-D for each group during the 5-minute training trial (One-way ANOVA: P > 0.05 within all age groups). (**e**) Sampling times for the 'switched' pair (Novel) vs the stationary pair. Prepubescent females and adult males sampled the 'switched' pair more than the stationary pair (2-tailed paired t-test: Prepub female **P = 0.008, Adult male ****P = 0.00004). Prepubescent male and adult females showed no preference (P = 0.65, P = 0.97, respectfully; N = 8-11). (f) *Left*. Schematic of the 'What' task (see Methods). *Right*. Sampling times for each odor (One-way ANOVA: P > 0.05 within all age groups; N = 8-9/group). (**g**) Sampling times for novel odor vs mean of the three familiar odors (2-tailed paired *t*-test: ***P < 0.001, **P < 0.01; N = 8-9/group). Data are represented as mean ± SEM. Detailed statistics are found in Supplementary Table 1.

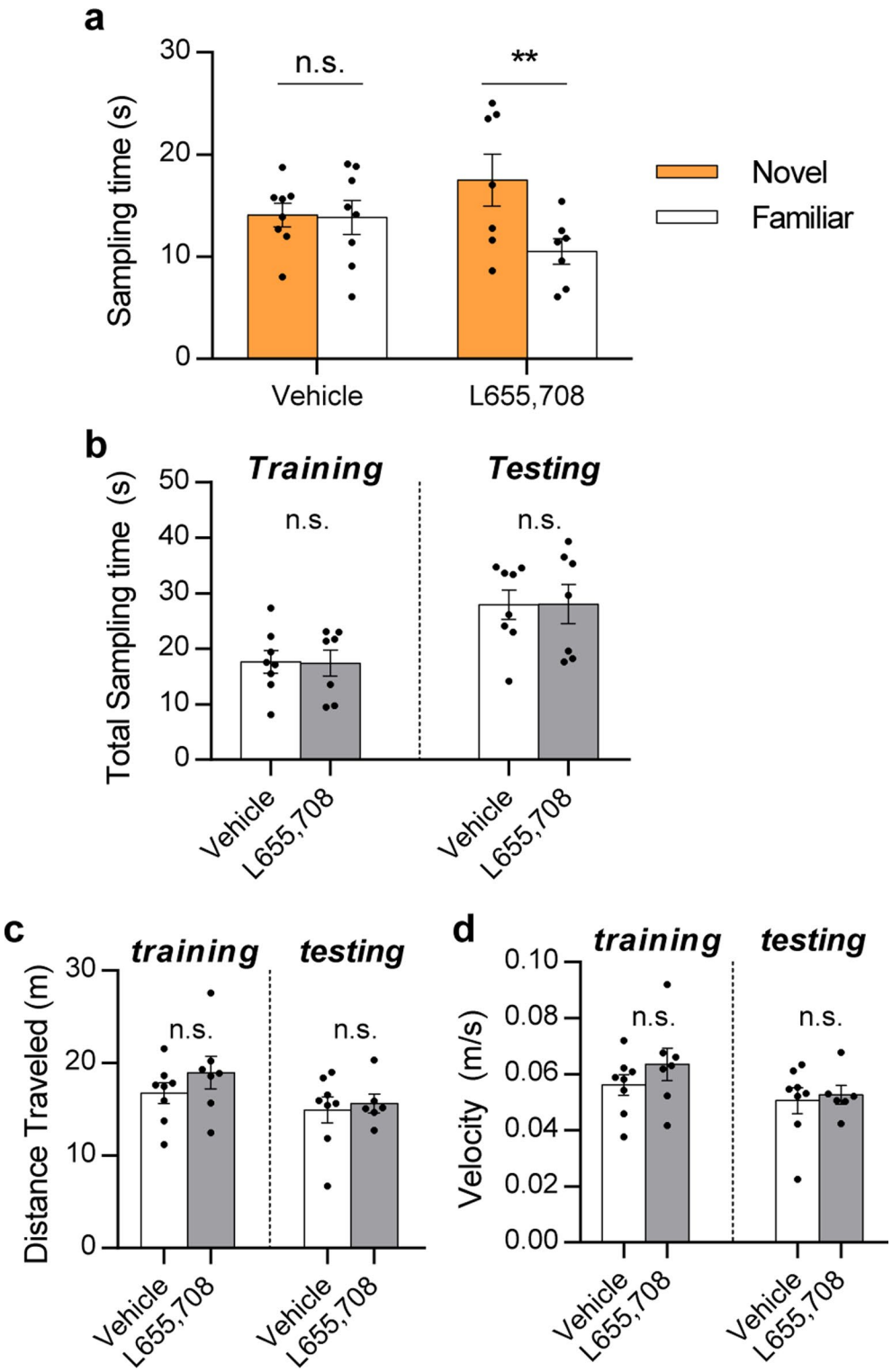

Extended Data Fig. 2 | Exploration data for 24-hour delay Object Location Memory in adult, non-proestrus female mice given L655,708. (**a**) Sampling times for displaced (Novel) vs stationary (Familiar) object for Vehicle (2-tailed paired t-test: n.s. P = 0.85) and L655,708 (**P = 0.009). (**b**) Total sampling times for training and testing were comparable for treated vs. vehicle groups (2-tailed unpaired t-test: n.s. training P = 0.95, testing P = 0.98). (**c**) Distance traveled was comparable (2-tailed unpaired t-test: training P = 0.29, testing P = 0.71) and (**d**) velocity was similar between treatments (training P = 0.30, testing P = 0.73). For all panels, Vehicle N = 8, L655,708 N = 7. Data presented as mean ± SEM. Further statistics found in Supplementary Table 1.

nature research

Corresponding author(s): Drs. Gary Lynch and Christine M. Gall

Last updated by author(s): Nov 22, 2021

Reporting Summary

Nature Research wishes to improve the reproducibility of the work that we publish. This form provides structure for consistency and transparency in reporting. For further information on Nature Research policies, see our Editorial Policies and the Editorial Policy Checklist.

Statistics

For all statistical analyses, confirm that the following items are present in the figure legend, table legend, main text, or Methods section.

n/a	Confirmed
☐	☒ The exact sample size (*n*) for each experimental group/condition, given as a discrete number and unit of measurement
☐	☒ A statement on whether measurements were taken from distinct samples or whether the same sample was measured repeatedly
☐	☒ The statistical test(s) used AND whether they are one- or two-sided *Only common tests should be described solely by name; describe more complex techniques in the Methods section.*
☐	☒ A description of all covariates tested
☐	☒ A description of any assumptions or corrections, such as tests of normality and adjustment for multiple comparisons
☐	☒ A full description of the statistical parameters including central tendency (e.g. means) or other basic estimates (e.g. regression coefficient) AND variation (e.g. standard deviation) or associated estimates of uncertainty (e.g. confidence intervals)
☐	☒ For null hypothesis testing, the test statistic (e.g. *F*, *t*, *r*) with confidence intervals, effect sizes, degrees of freedom and *P* value noted *Give P values as exact values whenever suitable.*
☒	☐ For Bayesian analysis, information on the choice of priors and Markov chain Monte Carlo settings
☒	☐ For hierarchical and complex designs, identification of the appropriate level for tests and full reporting of outcomes
☒	☐ Estimates of effect sizes (e.g. Cohen's *d*, Pearson's *r*), indicating how they were calculated

Our web collection on statistics for biologists contains articles on many of the points above.

Software and code

Policy information about availability of computer code

Data collection	Commercial data collection software Neurodata Acquisition System 2.0 (Theta Burst Corp.) was used to collect recordings in field slice electrophysiology. Whole-cell electrophysiology data was collected with Clampex 10.6 and analyzed with Clampfit 10.6 (Molecular Devices). Fluorescence Deconvolution Tomography (FDT) images were collected and deconvolved using Volocity 4.0.1 (Perkin Elmer). Statistical analysis was performed using Prism 6.0 (GraphPad).
Data analysis	Single and theta burst parameters for field electrophysiology were analyzed using code that can be found at https://github.com/cdcox/Theta-burst-analyzer-for-Le-et-al . FDT analysis uses in-house softwares which utilizes C99, Java (openJDK IcedTea6.1.12.6), Matlab R2019b, Perl v5.30.0, PuTTY 0.74). Code is made available upon reasonable request to the corresponding author. This has been previously described (Wang et al. 2018) by our group and has been represented in several publications including but not limited to: Rex et al., 2009; Babayan et al., 2012; Seese et al., 2014; Wang et al., 2016.

For manuscripts utilizing custom algorithms or software that are central to the research but not yet described in published literature, software must be made available to editors and reviewers. We strongly encourage code deposition in a community repository (e.g. GitHub). See the Nature Research guidelines for submitting code & software for further information.

Data

Policy information about availability of data

All manuscripts must include a data availability statement. This statement should provide the following information, where applicable:

- Accession codes, unique identifiers, or web links for publicly available datasets
- A list of figures that have associated raw data
- A description of any restrictions on data availability

The data that supports the findings of this study are available within the paper and its supplementary information files.

Field-specific reporting

Please select the one below that is the best fit for your research. If you are not sure, read the appropriate sections before making your selection.

☒ Life sciences ☐ Behavioural & social sciences ☐ Ecological, evolutionary & environmental sciences

For a reference copy of the document with all sections, see nature.com/documents/nr-reporting-summary-flat.pdf

Life sciences study design

All studies must disclose on these points even when the disclosure is negative.

Sample size	These values (group sizes) were determined by previous experience and power analysis. For electrophysiology studies, power analysis determined that the typical effect size and profile (change in response amplitude of 20% ; sigma=15; alpha=0.05; power=0.80) would require at minimum 5 slices/group for significance For behavioral experiments, power analysis determined that with an effect size (Discrimination Index) of 30% (sigma=10%; alpha=0.05; power=0.80), the minimum group size needed to detect a 10% difference in the DI would be 3 animals/group. For FDT experiments, power analysis determined that with the typical effect size and profile (change of 20%; sigma=15; alpha=0.05; power=0.80) studies would require a minimum of 5/group to determine significance.
Data exclusions	For behavioral analyses, measures from a particular animal were excluded if the measure for that animal were outside 4 standard deviations from the group mean, or if animal did not sample all cues during the behaviors. Using these standards, 1 animal was excluded for standard deviation reasons, and 8 animals were excluded from not sampling all cues. No electrophysiological results were excluded. No FDT results were excluded.
Replication	The number of animals in behavioral and FDT studies, or the number of independently evaluated hippocampal slices in electrophysiological studies, constituted an "N", and the N represented a replication which are provided in the figure legends. All studies (electrophysiology, FDT, and behavior) used at least 2 cohorts from different generation lines, and all replications were consistent and successful.
Randomization	For electrophysiological studies, each animal was used to prepare hippocampal slices that were randomly distributed amongst adjacent, identical recording rigs that received either vehicle (Rig #1) or drug (Rig #2) infusion simultaneously; because slice preparation and recordings were conducted simultaneously, there were no differences in temporal factors that might have affected the health of the slice. Moreover for the electrophysiological studies, the aCSF (tissue bath) solutions were prepared in sufficient volume to accomodate both rigs being run simultaneously so there were no differences in the chemical compositions. Age groups for electrophysiological or behavioral experiments were not randomized due to the age restriction (PND21-P28) of prepubescent group. Sex of the animal was randomized in appropriate experiments. For behavioral studies, the age groups were run simultaneously, and for injection studies, vehicle and drug was assigned randomly. For FDT studies, the variable was age and sex, therefore no randomization was needed beyond segregating into those groups. The tissue to be compared (from the different age/sex groups) was processed at the same time using the same solutions; images were collected at the same time and from coded microscope slices.
Blinding	For behavioral studies, the age of the animals were not blinded because the individual scoring the videos could see the size difference in prepubertal vs adult mice. However, the scorers were blind to (1) sex of the animals within each age group, (2) estrous cycle stage, (3) novel odor in the "What" and "Where paradigms, and (4) drug and vehicle injection groups. At least, two individuals scored the videos (blind to animal identity) independently to validate findings. For electrophysiological studies, it was not possible to blind for the animals age and sex, due to the visible differences in body weight and other appearance factors of the animal, and due to the need to check for estrous cycle. However, vaginal smears were not evaluated until after the experimental procedures were complete; consequentially estrous cycle stage was not known at the time of experiment but was determined afterwards. For FDT analysis, all slides were coded, processed, and imaged blind.

Reporting for specific materials, systems and methods

We require information from authors about some types of materials, experimental systems and methods used in many studies. Here, indicate whether each material, system or method listed is relevant to your study. If you are not sure if a list item applies to your research, read the appropriate section before selecting a response.

Materials & experimental systems

n/a	Involved in the study
☐	☒ Antibodies
☒	☐ Eukaryotic cell lines
☒	☐ Palaeontology and archaeology
☐	☒ Animals and other organisms
☒	☐ Human research participants
☒	☐ Clinical data
☒	☐ Dual use research of concern

Methods

n/a	Involved in the study
☒	☐ ChIP-seq
☒	☐ Flow cytometry
☒	☐ MRI-based neuroimaging

Antibodies

Antibodies used

Mouse anti-PSD95 (AB_325399; Thermo Fisher Scientific #MA1-045; 6G6-1C9 clone), Goat anti-PSD-95 (AB_298846; Abcam #ab12093), Rabbit anti-gephyrin (AB_1860490; Abcam # ab32206), Rabbit anti-α5-GABAAR (AB_296840; Abcam # ab10098), Mouse anti-α2-GABAAR (AB_2890213; Abcam #ab19331; N399/19 clone), Guinea pig anti-β1-GABAAR (AB_2619940; Synaptic Systems #224705), Mouse anti-gephyrin (AB_2232546; Synaptic Systems #147021; mAb7a clone), Guinea pig anti-vesicular GABA transporter (AB_887873; Synaptic Systems #131004), Rabbit anti-ERα (AB_631470; Santa Cruz Biotechnology; #sc-542), Mouse anti-ERβ (AB_2728765; Santa Cruz Biotechnology #sc-390243).

Secondary antibodies: donkey anti-rabbit Alexa Fluor 594 (AB_141637; Thermo Fisher Scientific #A-21207), goat anti-guinea pig Alexa Fluor 488 (AB_2534117; Thermo Fisher Scientific #A-11073), donkey anti-goat Alexa Fluor 488 (AB_2534102; Thermo Fisher Scientific #A-11055), and donkey anti-mouse Alexa Fluor 488 (AB_141607; Thermo Fisher Scientific #A-21202).

Validation

Mouse anti-PSD95 (AB_325399; Thermo Fisher #MA1-045; 6G6-1C9 clone). This monoclonal antibody has been widely used for labeling the excitatory postsynaptic density (>240 publications, with over 100 immunocytochemistry publications alone). It is well characterized including verification by western blotting and relative expression studies (Thermo Scientific).

Goat anti-PSD-95 (AB_298846; Abcam #ab12093): This polyclonal antibody has been cited by 49 publications and reacts to mouse, rat, and human tissue. Additionally, the vendor has verified the specificity (single band at ~95 kDa) through Western blot.

Rabbit anti-gephyrin (AB_1860490; Abcam # ab32206): This polyclonal antibody that has been cited by at least 19 publications and detects a primary band of ~90kD in rat and mouse brain tissue that corresponds to isoform 1 of gephyrin; in control studies by the vendor this labeling was partially blocked by the immunizing protein. Hales et al. 2013 verified the antibody specificity.

Rabbit anti-α5-GABAAR (AB_296840; Abcam # ab10098): This polyclonal antibody that has been cited by at least 16 publications and detects a primary band of ~52kD (predicted 55 kD) in mouse brain. It is KO-validated by Magnin et al. 2019. In the manuscript under review, our study shows an increase in synaptic GABAAR-α5 levels in the CA1 stratum radiatum in adult females vs prepubescent females. Importantly, in both acute field and patch clamp electrophysiology experiments, infusion of the GABAAR α5-negative allosteric modulator (L655,708) reduced the shunting inhibition of the adult females significantly more compared to prepubescent females in the same CA1 area thereby corroborating the prediction, from the immunofluorescence results, of greater GABAAR-α5 levels in the older group.

Mouse anti-α2-GABAAR (AB_2890213; Abcam #ab19331; N399/19 clone): This monoclonal antibody has been cited by 4 publications. Specificity of the antibody clone (N399/19), has been verified in KO studies (EMD Millipore) and by the demonstration that it is not cross-reactive with α1-GABAAR (EMD Millipore).

Guinea pig anti-β1-GABAAR (AB_2619940; Synaptic Systems #224705): This affinity purified antibody recognizes the predicted ~55 kD band from synaptic membrane fractions of rat brain, and colocalizes with GABAA receptor gamma 2 (as expected for ß1) in inhibitory synapses in EM studies (Kerti-Szigeti and Nusser 2016).

Mouse anti-gephyrin (AB_2232546; Synaptic Systems # 147021; mAb7a clone): Monoclonal antibody specific for the brain specific 93 kD spice variant; the specificity has been KO verified by the vendor. It has been used in over 60 publications (46 for immunolabeling).

Guinea pig anti-vesicular GABA transporter (AB_887873; Synaptic Systems # 131004): polyclonal antibody that has been used in over 100 publications and has been KO verified by the vendor.

Rabbit anti-ERα (AB_631470; Santa Cruz Biotechnology; #sc542); widely used polyclonal antibody for ERα (used in 295 publications). Highly specific for ~66 kD long isoform band of ERα, and KO verified by Matic et al. 2013 and Collins et al. 2018.

Mouse anti-ERβ (AB_2728765; Santa Cruz Biotechnology #sc-390243); This monoclonal antibody for ERβ has been cited in 21 publications. Highly specific for ~56 kD (predicted) band of ERβ, and intensely labels human testes. Verified by Troncoso et al. 2020 for Western blot (~60 kDa) and does not cross-react with ERα.

Donkey anti-rabbit Alexa Fluor 594 (AB_141637; Invitrogen, Thermo Fisher Scientific cat # A-21207). This is a highly crossed absorbed secondary antibody with a well-characterized specificity for rabbit immunoglobulins, and has been cited in 147 publications.

Goat anti-guinea pig Alexa Fluor 488 (AB_2534117; Invitrogen, Thermo Fisher Scientific cat # A-11073). This is an affinity purified and highly crossed absorbed secondary antibody with a well-characterized specificity for guinea pig immunoglobulins, and has been cited in 77 publications.

Donkey anti-goat Alexa Fluor 488 (AB_2534102; Invitrogen, Thermo Fisher Scientific cat # A-11055). This is a highly crossed absorbed secondary antibody with a well-characterized specificity for goat immunoglobulins, and has been cited in 229 publications.

Donkey anti-mouse Alexa Fluor 488 (AB_141607; Invitrogen, Thermo Fisher Scientific cat # A-21202). This is a highly crossed absorbed secondary antibody with a well-characterized specificity for goat immunoglobulins, and has been cited in 315 publications.

Animals and other organisms

Policy information about studies involving animals; ARRIVE guidelines recommended for reporting animal research

Laboratory animals	This studies presented in the manuscript used Sprague-Dawley male and female rats (post-natal day 21-28 and 2-3 month old) and sighted-FVB129 male and female mice (post-natal day 21-25 and 2-4 month old).
Wild animals	None
Field-collected samples	None
Ethics oversight	Experiments were performed in accord with NIH guidelines for the Care and Use of Laboratory Animals and protocols approved by Institutional Animal Care and Use Committee at University of California, Irvine.

Note that full information on the approval of the study protocol must also be provided in the manuscript.